

Review

Image-Based High-Throughput Phenotyping in Horticultural Crops

Alebel Mekuriaw Abebe, Younguk Kim, Jaeyoung Kim, Song Lim Kim and Jeongho Baek *

Department of Agricultural Biotechnology, National Institute of Agricultural Science, Rural Development Administration, Jeonju 54874, Republic of Korea

* Correspondence: firstleon@korea.kr; Tel.: +82-63-238-4670

Abstract: Plant phenotyping is the primary task of any plant breeding program, and accurate measurement of plant traits is essential to select genotypes with better quality, high yield, and climate resilience. The majority of currently used phenotyping techniques are destructive and time-consuming. Recently, the development of various sensors and imaging platforms for rapid and efficient quantitative measurement of plant traits has become the mainstream approach in plant phenotyping studies. Here, we reviewed the trends of image-based high-throughput phenotyping methods applied to horticultural crops. High-throughput phenotyping is carried out using various types of imaging platforms developed for indoor or field conditions. We highlighted the applications of different imaging platforms in the horticulture sector with their advantages and limitations. Furthermore, the principles and applications of commonly used imaging techniques, visible light (RGB) imaging, thermal imaging, chlorophyll fluorescence, hyperspectral imaging, and tomographic imaging for high-throughput plant phenotyping, are discussed. High-throughput phenotyping has been widely used for phenotyping various horticultural traits, which can be morphological, physiological, biochemical, yield, biotic, and abiotic stress responses. Moreover, the ability of high-throughput phenotyping with the help of various optical sensors will lead to the discovery of new phenotypic traits which need to be explored in the future. We summarized the applications of image analysis for the quantitative evaluation of various traits with several examples of horticultural crops in the literature. Finally, we summarized the current trend of high-throughput phenotyping in horticultural crops and highlighted future perspectives.

Keywords: phenotyping; image analysis; phenomics; sensor; horticultural crop



Citation: Abebe, A.M.; Kim, Y.; Kim, J.; Kim, S.L.; Baek, J. Image-Based High-Throughput Phenotyping in Horticultural Crops. *Plants* **2023**, *12*, 2061. <https://doi.org/10.3390/plants12102061>

Academic Editor: Georgios Koubouris

Received: 12 April 2023

Revised: 12 May 2023

Accepted: 18 May 2023

Published: 22 May 2023



Copyright: © 2023 by the authors. Licensee MDPI, Basel, Switzerland. This article is an open access article distributed under the terms and conditions of the Creative Commons Attribution (CC BY) license (<https://creativecommons.org/licenses/by/4.0/>).

1. Introduction

The world population keeps increasing and is expected to reach ten billion by 2050, so as the demand for food and energy. This alarms the need to maximize the yield and quality of food crops as well as reduce postharvest losses. Breeding for high yield, better quality, and resistance to biotic (disease, pest, weed) and abiotic (drought, salt, heat, cold) stresses should be the priority to meet the projected food demand. Plant phenotyping is the core of any plant breeding program, and accurate measurement of plant traits is essential for the selection of the best genotypes. Phenotype is the result of the interactions between genotype and all the surrounding environmental conditions during the plant growth cycle, whereas phenotyping refers to the measurement of any aspect of plant traits, including growth, development, and physiology [1]. Plant phenomics is the high-throughput collection and analysis of multidimensional phenotypes of the whole plant through its life span [2,3]. The advancement of next-generation sequencing and marker technology has accelerated genomic study, allowing the mapping and identification of genes controlling complex traits [4]. However, phenomic information is not adequately available due to the effect of environmental factors and lack of accurate measurements limiting the phenotypic characterization of crop traits.

Conventional phenotyping has been the bottleneck for breeding for a long time as it is labor-intensive, time-consuming, and does not have high throughput [5]. The recent introduction of high-throughput phenotyping methods is accelerating plant phenotyping, enabling high-throughput measurement of several phenotypic data nondestructively and objectively [3,6]. Furthermore, high-throughput phenotyping with the help of optical sensors, computer vision, and robotics will bring new traits under consideration which were difficult to measure via the conventional method.

High-throughput phenotyping platforms can image hundreds of plants daily using various types of optical sensors, allowing the measurement of morphological, physiological, biochemical, and performance traits in a non-destructive way [7–10]. The principle of image-based phenotyping is based on the interaction of electromagnetic radiation and the plant surface, including absorption, reflection, emission, transmission, and fluorescence, which differ between normal and stressed plants or among genotypes [9]. These interactions will help to estimate various types of phenotypic traits of the plant with the help of optical sensors. Image-based high-throughput phenotyping aims to quantify numerous traits, which requires the use of various types of optical sensors. Some of the currently available sensors for plant phenotyping include visible light (red–green–blue), thermal, fluorescence, hyperspectral, multispectral, light detection and ranging (LiDAR), magnetic resonance (MRI) imaging, X-ray computed tomography (X-ray CT), and positron emission tomography (PET) [3,11,12]. The applications of various types of sensors may differ depending on imaging platforms, accessibility, cost, and the target trait under consideration. The different sensors can be used separately or in combination for fast and accurate plant phenotyping, each of which comes with its own advantages and limitations.

High-throughput phenotyping is used in breeding, crop cultivation, and even postharvest, depending on the purpose of phenotyping. In plant breeding, phenotyping a large number of samples (population) aims to increase the selection intensity and accuracy and characterize various crop traits to select the best genotypes, while phenotyping in crop cultivation is used to monitor the occurrence of any plant stresses such as disease, pests, nutrient stress, weeds, or abiotic stress at early stages [1,8]. Real-time phenotypic data acquisition and analysis will help to make immediate management decisions for the crop. Hence, image-based phenotyping will play a pivotal role in the precision cultivation of horticultural crops. Horticultural crops are mostly utilized in the fresh state and are highly perishable due to their high water content, such as vegetables and fruits. The market value of horticultural products is highly dependent on external appearance (color, shape, size, texture) and internal (soluble solid content and firmness) quality attributes. The status of these quality attributes changes over time during maturity, ripening, and postharvest storage and should be routinely monitored [13,14]. Currently, external quality attributes are mostly evaluated using visual inspection in the horticulture chain, which is slow and subjective. On the other hand, internal quality attributes are quantified using destructive laboratory analysis or handheld/portable instruments, which are also limited in speed and sample size. Due to the highly perishable nature and the dynamics of quality attributes over time in horticultural products, image-based phenotyping will greatly improve the speed, volume, and accuracy of postharvest phenotyping.

In this paper, we reviewed the applications of image-based phenotyping for the assessment of various traits in horticultural crops. Commonly used imaging platforms and sensors for high-throughput phenotyping are described. The application of these technologies for phenotyping various traits of horticultural crops is discussed with several examples in the literature. Finally, the current trends and future perspectives of high-throughput phenotyping in horticultural crops are highlighted. Using multiscale imaging platforms equipped with state-of-the-art imaging technologies will enable rapid and accurate quantitative measurement of diverse plant phenotypic traits to accelerate crop improvement, precision agriculture, and objective postharvest phenotyping (Figure 1).

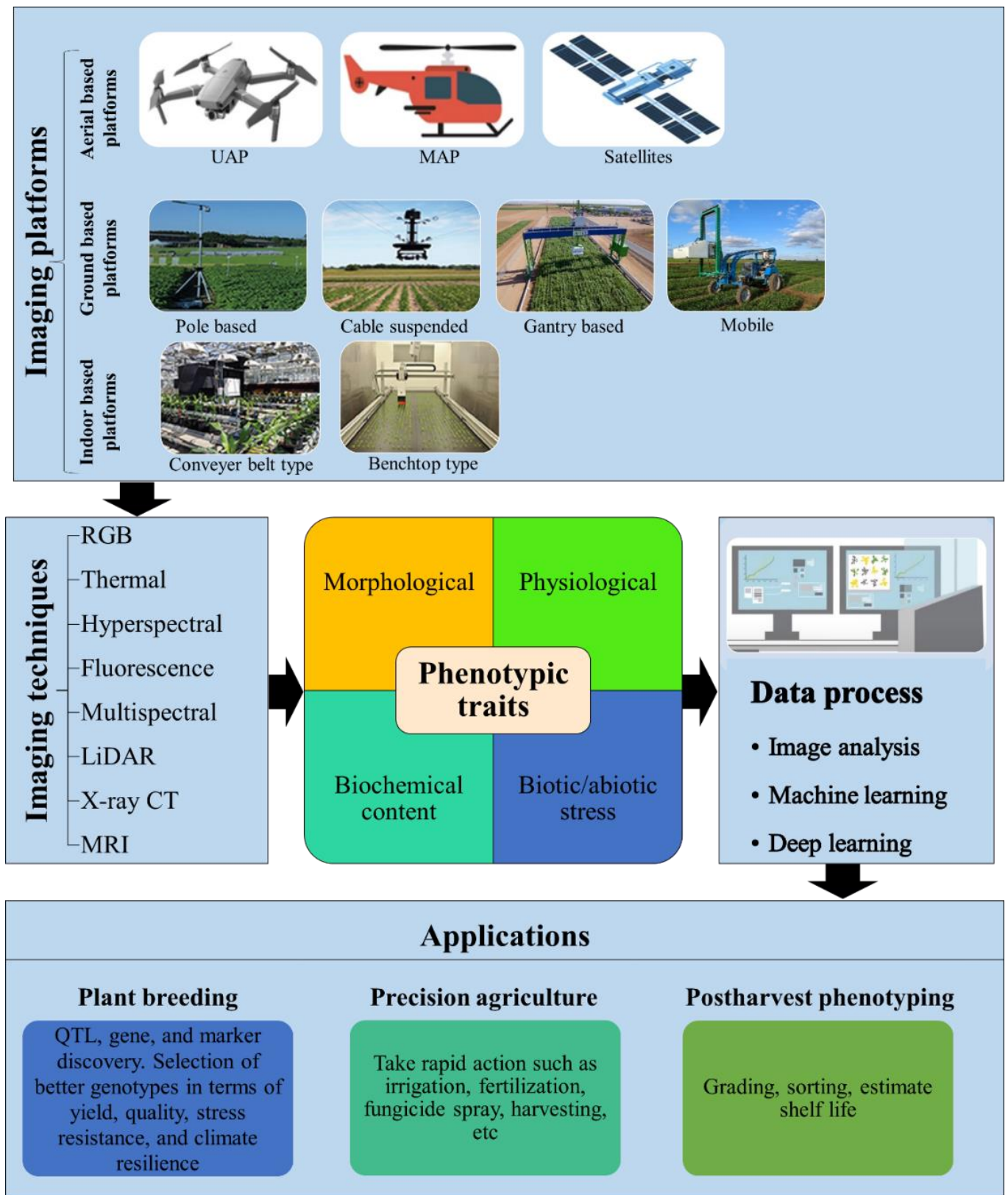


Figure 1. Schematic overview of image-based high-throughput phenotyping in horticultural crops. UAP, unmanned aerial platform; MAP, manned aerial platform; RGB, red–green–blue; LiDAR, light detection and ranging; X-ray CT, X-ray computed tomography; MRI, magnetic resonance imaging.

2. High-Throughput Phenotyping Platforms

High-throughput phenotyping is carried out using various types of imaging platforms. The suitability of high-throughput phenotyping platforms may vary depending on the imaging environment, e.g., laboratory, growth chamber, greenhouse, or field. In most controlled environment conditions, imaging is carried out by moving the sensor towards the plant (sensor movement type) or the plant is transported to the fixed imaging setup using a conveyer belt or other transporting methods (plant movement type) for routine phenotypic measurement. For example, a greenhouse-based sensor-to-plant platform was used to measure static and dynamic traits such as geometric, structural, color, and textural phenotypes of lettuce [15]. Image-based phenotyping in controlled environment conditions has the advantage of high precision, high repeatability, continuous automated operation, and absence of interference from external environmental conditions. However, they are generally expensive and can monitor a very limited number of samples. The conveyer type and benchtop-type platforms are mostly used and have well-established systems for controlled environment conditions [6].

Imaging platforms for field-based conditions can be ground or aerial-based, targeting phenotyping of plant characteristics at individual plant or area levels. They are grouped into ground-based or aerial-based on the structures where the sensor is mounted. Ground-based imaging platforms such as pole/tower-based, mobile platform (vehicle), gantry-based, and cable suspended are flexible for deployment and have a good spatial resolution. However, they are subject to varying environmental conditions due to the slow speed of covering a large field. Aerial-based imaging platforms include unmanned aerial platforms, manned aerial platforms, and satellites. These imaging platforms can cover a wide area in a short period of time and are able to overcome varying environmental conditions. The disadvantage of the platforms is that they have a limited payload, and the spatial resolution of the image is affected by the speed and altitude of the aerial structure [6,9]. Unmanned aerial vehicle (UAV) platforms were used for the measurement of various traits in horticultural crops. For example, UAV-based remote sensing coupled with different machine learning approaches was used for disease detection and classification in potato, tomato, banana, pear, and apple [16–22], for tree detection in orchards such as banana and citrus [23–25], for aboveground biomass estimation in onion, potato, tomato, and strawberry [26–29], and other traits of fruits and vegetables [23,30,31].

3. Commonly Used Imaging Techniques for High-Throughput Plant Phenotyping

3.1. Visible Light Imaging

Visible light sensors detect light in a wavelength spectrum of 400–700 nm and provide reflected values of red, green, and blue (RGB). Visible light imaging is widely used for high-throughput phenotyping because of its accessibility, simplicity, and low cost [32]. High-resolution RGB images can be used to accurately measure plant biomass [28,33–37], root architecture [38,39], plant growth rate [40–43], germination rate [44], yield [45–47], disease detection and quantification [17,48–50], and abiotic stresses [51]. Their application in the field can be affected by minimal color variation between the leaf and the background and the influence of light for automatic image processing [32].

3.2. Thermal Imaging

Thermal infrared imaging allows the visualization and distribution of infrared radiation over a leaf or plant surface. A thermal camera converts infrared radiation (heat) emitted from the object into visible images showing the spatial distribution of surface temperature. The thermal sensor records the emitted light from the object in the thermal range of 3–5 μm or 7–14 μm with an image showing the temperature values per pixel. Thermal imaging can be used to detect the physiological status of the plant in response to biotic and abiotic stress, such as canopy or leaf temperature [52], transpiration and stomatal conductance [53], and plant water status [9,11]. Under water deficit conditions, plants

close their stomata and reduce water loss through transpiration which is also highly linked with the soil moisture content. The reduction in transpirational cooling results in increased leaf temperature. Hence, thermal imaging can be used to manage water and irrigation in precision agriculture [54].

3.3. Hyperspectral Imaging

Hyperspectral imaging captures electromagnetic spectra (λ) and spatial (x, y) data at every pixel in an image to reconstruct the 3D data matrix called hypercube, containing thousands of images in the spectral range of 250–2500 nm encompassing UV, VIS, NIR, and SWIR [55]. It offers a large amount of information, allowing the extraction of a wide range of phenotypic traits, while the storage and analysis of the vast amount of hyperspectral data is challenging. Some of its applications include estimation of nutrient content, disease detection [16,56–58], fruit maturity and ripening [59,60], and other physiological and biochemical traits which are used to infer plant growth and development as well as yield [55].

3.4. Fluorescence Imaging

The light energy absorbed by chlorophyll can be used for photosynthesis, dissipated as heat, or re-emitted. Fluorescence is the light emitted when the plant absorbs radiation of shorter wavelengths, mainly via the chlorophyll complex, and is very small (<3%) compared to the total amount of radiation emitted to the object from the light sources. The amount of re-emitted light (fluorescence) is a good indicator of the plant's ability to utilize the absorbed light and is used to estimate the overall plant health status [61]. Fluorescence imaging is used to estimate photosynthetic efficiency and other associated metabolic processes of the plant affected by biotic and abiotic stresses [62–65]. The fluorescence pattern of plants under stress conditions will show an altered pattern compared to non-stressed plants. Sensors sensitive to fluorescence are used to capture fluorescence signals after illumination of the plant or tissue with visible light, infrared, or UV light. Maximum quantum efficiency (F_v/F_m), non-photochemical quenching (energy dissipated as heat from photosynthetic reaction center), the effective quantum yield of PSII (Φ_{PSII} or F_q'/F_m'), and relative electron transport rate are some of the parameters derived from chlorophyll fluorescence which are used to assess the physiological status of the plant in relation to different stress conditions, where F_m is maximum fluorescence of a dark-adapted leaf and F_v is the difference between F_m and minimum fluorescence from dark-adapted leaf (F_0) [10]. The problem with fluorescence imaging in the field condition is that it does not specify the cause of signal changes in the plant, e.g., light, temperature, or other environmental factors [11,61].

3.5. Tomographic Imaging

Other imaging techniques such as magnetic resonance imaging (MRI), X-ray computed tomography (X-ray CT), and positron emission tomography (PET) provide high-resolution 3D images of a single plant or plant parts [66]. MRI captures the 3D images of the internal structures of the sample enabling non-invasive quantification of both static and dynamic traits such as structural, biochemical, and temporal changes inside the plant. MRI can be used to monitor changes in growth and development (seed and bulb germination, seed development, fruit growth, and root growth), water dynamics within the plant, drought stress responses (drought stress, salt stress, cold stress, and heat stress), and the plant–pathogen interaction [67]. X-ray CT is used to visualize the 3D structures of internal and external features of the plant at the micro or macro level. When the X-ray beam passes through the sample, part of the beam is absorbed, and the remaining radiograph is recorded by the detector. Multiple 2D projections are recorded by moving the sample or the sensor, which are then used to reconstruct the 3D images [68]. For example, it has been used for the characterization of size and shape-related morphological traits of seed and fruit [69,70]. These imaging techniques

are time-consuming and are not suitable when a large number of samples are under consideration. In addition, due to the larger size and heavy weight of the equipment it is not usable on aerial imaging platforms [55]. Examples of images from commonly used sensors in high-throughput phenotyping are shown in Figure 2.

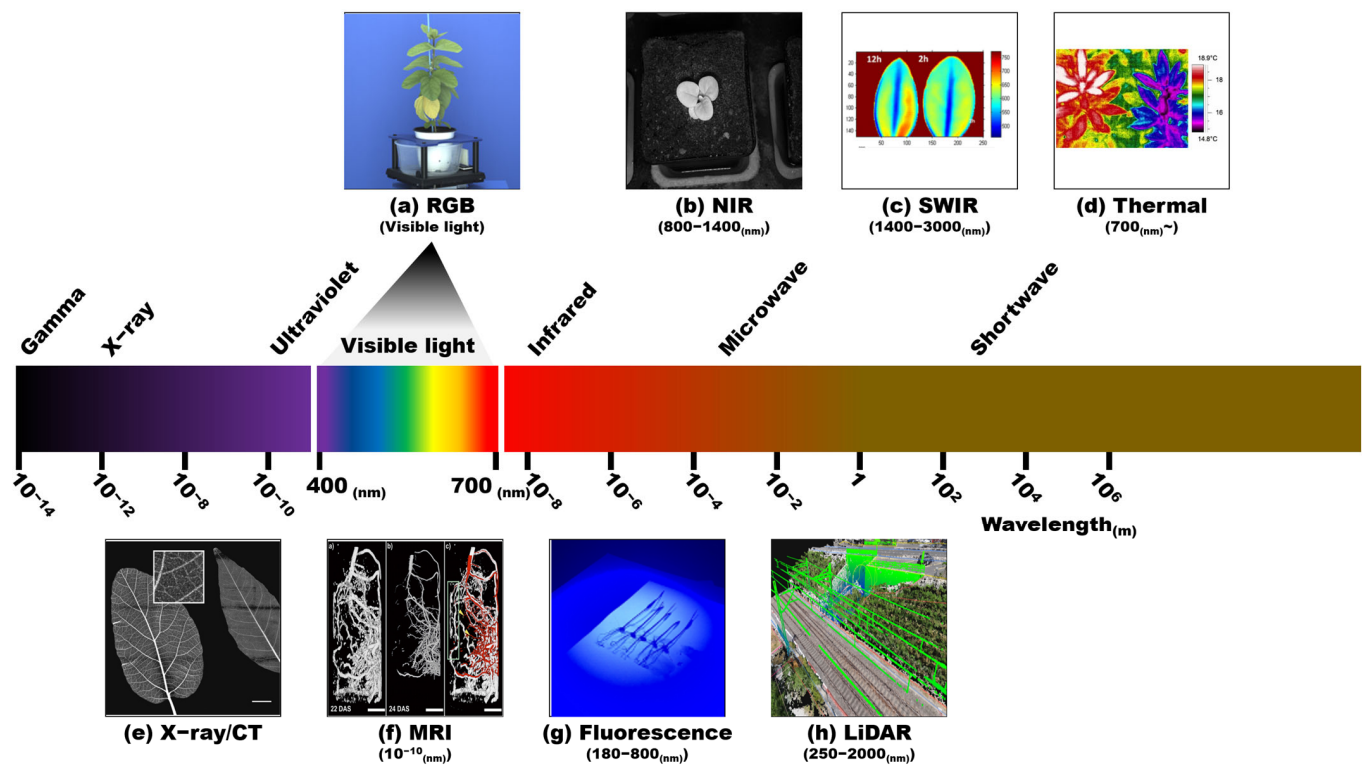


Figure 2. Examples of images from commonly used sensors in high-throughput phenotyping and their spectral range. (a) RGB; (b) NIR [71]; (c) SWIR [72]; (d) thermal (Qubit phenomics, Canada); (e) X-ray [73]; (f) MRI [66]; (g) fluorescence; (h) LiDAR and photogrammetry point cloud (Pix4D S.A., Prilly, Switzerland). RGB and fluorescence images were captured in our lab.

Imaging technology is the primary component of high-throughput plant phenotyping as acquired phenotypic traits are determined by the type of sensor (imaging technique). Visible light (RGB) imaging and multi/hyperspectral imaging techniques are widely used to acquire morphological, physiological, biochemical, biotic, and abiotic stress-related traits. Fluorescence imaging and thermal imaging are used to capture the photosynthetic and surface temperature of the plant, respectively, which are physiological traits. LiDAR, X-ray CT, and MRI are mainly used to acquire morphological traits [3]. Different imaging techniques come with their specific advantages and disadvantages to capture certain plant traits. The summary of imaging techniques and measurable phenotypic traits with potential applications in high-throughput plant phenotyping is presented in Table 1. Among the variety of commercially available sensors for different imaging techniques, the choice depends on the cost, robustness, and other specifications of the sensor to capture the target trait [74]. Examples of different sensors used for high-throughput phenotyping of some horticultural crops are presented in Table 2. High-throughput phenotyping will benefit from the increasing capabilities and advancements of sensor technologies.

Table 1. Summary of most common imaging techniques used in high-throughput plant phenotyping [11,75].

| Imaging Technique ^a | Phenotypic Traits | Advantages | Limitations | Potential Applications |
|--------------------------------|---|--|---|--|
| Visible light imaging | Shape, color, size, biomass, pigment content, disease and pest, stress responses, nutrient stress, vegetation indices | Cheap, easy operation and maintenance, provide color information, high resolution, fast data acquisition | Limited to three spectral bands (RGB), affected by light, only provide relative measurement | Growth monitoring, plant stress detection, fruit maturity and ripening estimation, grading and sorting, quality evaluation, yield prediction, 3D modeling, crop management, robotic harvesting |
| Thermal imaging | Leaf greenness, leaf color, leaf chlorophyll content, leaf/canopy temperature, disease and pest, phenology, photosynthetic status | Wide measurement range, background interference can be removed | Require sensor calibration and atmospheric correction, difficulty of through time comparison due to changes in ambient condition affecting canopy temperature, need reference for comparison, difficult to separate soil and plant temperature in sparse canopies (limiting the automation of image processing) | Plant stress detection, irrigation scheduling |
| Hyperspectral imaging | Leaf/canopy water status, canopy coverage and volume, leaf greenness, disease and pest, photosynthetic rate, nutrient stress, metabolites | High spectral resolution, background interference can be removed | Expensive, low spatial resolution, too large image data challenging for storage and analysis, affected by ambient light condition | Growth monitoring, biotic and abiotic stress detection, fruit maturity and ripening estimation, quality evaluation, biomass estimation, metabolite prediction |
| Fluorescence imaging | Chlorophyll content, canopy coverage, disease and pest, photosynthetic status | Sensitive to fluorescence and water stress | Limited in field application, difficult to measure at the canopy scale due to the small signal-to-noise ratio | Growth monitoring, early detection of biotic and abiotic stress |
| Multispectral imaging | Canopy coverage and volume, chlorophyll content, leaf greenness, plant diseases and pests, photosynthetic status, water content | Easy in image processing; mature technology | Limited to several spectral bands; spectral data should be frequently calibrated using referenced objects; effects of camera geometrics, illumination condition, and sun angle on the data signal | Growth monitoring, biotic and abiotic stress detection |
| LiDAR | Plant height, canopy volume, shoot biomass | Provide three-dimensional shape | Expensive, sensitive to the small difference in path length; specific illumination required for some laser scanning instruments, data processing is time-consuming | Growth monitoring, structure capture |

Table 1. *Cont.*

| Imaging Technique ^a | Phenotypic Traits | Advantages | Limitations | Potential Applications |
|--------------------------------|---|---|--|--|
| 3D laser scanner | Geometrical plant traits such as shape, length, height, canopy structure and volume | Long measurement distance; high precision; good penetration | Expensive, affected by external factors such as wind and fog | Growth monitoring, organ morphogenesis |
| MRI | Internal structures, metabolites, development of root systems, water presence | Available for screening 3D structural information | Expensive, low throughput, slow data acquisition | Acquire 3D structures of the whole plant or plant parts |
| X-ray CT | Size and shape | Large penetration depth, scalable field of view, minimal sample preparation | Expensive, low throughput | Growth monitoring, seed and fruit development, organ morphogenesis, 3D visualization of plant organs and tissues |

^a Imaging technique: LiDAR—light detection and ranging; MRI—magnetic resonance imaging; X-ray CT—X-ray computed tomography.

Table 2. Examples of sensors used for different imaging techniques in high-throughput plant phenotyping.

| Imaging Technique | Sensor (Manufacturer) | Resolution | Crop | Reference |
|-----------------------|---|----------------|------------|-----------|
| Visible light imaging | DJI Phantom 4 Pro (DJI Technology Co., Shenzhen, China) | 3000 × 4000 px | Strawberry | [76] |
| | Sony Cyber-shot DSC-H3 camera (Sony Corporation, Tokyo, Japan) | 3264 × 2448 px | Tomato | [38] |
| | Fujifilm X20 (Fujifilm Corporation, Tokyo, Japan) | 3000 × 4000 px | Apple | [77] |
| Thermal imaging | 3DR Solo quadcopter (3D Robotics, Berkeley, CA, USA) | 1280 × 960 px | Banana | [23] |
| | Vario CAM hr inspect 575 (Jenoptic, Jena, Germany) | 768 × 576 px | Mango | [78] |
| Hyperspectral imaging | Pika L 2.4 (Resonon Inc., Bozeman, MT, USA) | unknown | Tomato | [58] |
| | HySpex VNIR 1800, HySpex SWIR 384 (Norsk Elektro Optikk A/S, Skedsmokorset, Norway) | unknown | Grape | [79] |
| Fluorescence imaging | PlantScreen TM Transect XZ system (Photon Systems Instruments, Drásov, Czech Republic) | 1360 × 1024 px | Lettuce | [64] |
| Multispectral | Parrot Sequoia camera (Parrot Drone SAS, Paris, France) | 1280 × 960 px | Banana | [80] |
| | RedEdge-M, (MicaSense, Seattle, WA, USA) | 1280 × 960 px | Citrus | [81] |
| LiDAR | PlantEye F400 (Phenospex, Heerlen, The Netherlands) | unknown | Potato | [82] |
| 3D laser scanner | FARO Focus 3D 120 terrestrial laser scanner (Faro Technologies Inc., Lake Mary, FL, USA) | 1/5 | Cassava | [83] |
| X-ray CT | X-ray imaging system (Xeye-5100F, SEC, Suwon, Republic of Korea) | 2304 × 1300 px | Watermelon | [70] |

4. Applications of Image-Based High-Throughput Phenotyping in Horticultural Crops

4.1. Measurement of Morphological Traits

The morphological traits, including color, size, shape, and surface texture, determine the appearance of the produce and are used as quality parameters for visual inspection of horticultural crops. Although visual evaluation is a widely used nondestructive method for grading and sorting in horticultural crops, utilization of high-throughput phenotyping platforms is essential to obtain robust, faster, and objective results [14]. Nowadays, quantitative measurement of these traits (color, size, shape, and surface texture) using image analysis is increasingly used in different horticultural crops [13,84–87].

For example, grape berry color is a very important trait in grape breeding, which is qualitatively classified into six classes (green, yellow, rose, red, grey, dark red violet, or blue-black) according to the International Organization of Vine and Wine [88] or simply as noir (red, blue, or black) and non-noir (green or white). However, a qualitative assessment is very difficult to differentiate between noir and non-noir groups. Image-based phenotyping using different color spaces, RGB (red–green–blue), L^*a^*b (lightness, red–green, blue–yellow), and HSI (hue, saturation, intensity), allows for the easy discrimination of grape berry genotypes with different colors. RGB and HSI are able to separate within the noir and non-noir groups and enable the identification of minor QTLs controlling grape berry color, which were not identified previously using qualitative evaluation [89]. Quantitative measurement of strawberry fruit shape based on elliptic Fourier descriptors (EFDs) [90] and image analysis allowed the identification of two QTLs for shape via a genome-wide association study [84]. The fruit shape was highly correlated with the fruit length-to-width ratio.

The application of computer vision for shape quantification using images of sweet potatoes has shown that shape features, length-to-width ratio, curvature, cross-section roundness, and cross-sectional diameters, are highly predictive of shape classes. A neural network-based shape classifier was able to predict marketable (high market value) and non-marketable sweet potato classes with 84.59% accuracy [13]. In most food industries, quality is mainly assessed by experts based on subjective evaluation, which is very slow and inconsistent. The application of image-based phenotyping in the food industry is very important for fast, reliable, and objective evaluation. The browning of apple slices was quantified using color space, L^*a^*b , and textural features (entropy, contrast, and homogeneity) from the RGB images taken over time and showed that cv. Golden Delicious has less browning compared to Honey Crispy and Granny Smith [87].

In most horticultural crops, color, size, and texture are used as indicators of maturity and ripening. The maturity and ripening of plum and banana fruits were estimated based on these features using image analysis in which color was the dominant feature for the classification of maturity and ripening levels [91,92]. In general, color, size, shape, and texture are used to evaluate the external qualities of horticultural crops that greatly affect the market value of the produce. The applications of these quality attributes for the assessment of external qualities of horticultural crops based on hyperspectral imaging were previously reviewed [14].

4.2. Measurement of Physiological Traits

Physiological traits indicate the processes that occur within the plant, such as photosynthesis, transpiration, and canopy temperature. These traits determine how the plant is functioning under certain environmental conditions and are used to characterize the plant response to biotic and abiotic stresses, plant growth, and plant development [3]. Physiological traits can be quantified using various types of sensors, including RGB, ChlF, multispectral/hyperspectral, and thermal.

In horticultural crops, the physiological processes continue after harvesting (postharvest physiology). Postharvest physiology deals with the response of horticultural produce during postharvest storage and handling conditions along the processing or marketing chain. It determines the ripening, shelf life, and the quality of the produce. Due to their

highly perishable nature, the quality and shelf life of horticultural crops is dependent on pre/postharvest handling and storage conditions [14]. Hence, high-throughput postharvest phenotyping is necessary for rapid, robust, and accurate measurement of ripening, shelf life, quality, food safety, and biochemical contents of the horticultural produce [86]. This will help to track the physiological status of the produce and make immediate decisions to avoid economic losses. For example, visual inspection and analytical methods such as spectroscopy and HPLC (high-performance liquid chromatography) analysis are widely used for fruit quality assessment, which is labor-intensive, destructive, time-consuming, and not robust. Therefore, using high-throughput methods which can accurately and efficiently measure fruit and vegetable quality attributes is essential. Chilling injury, one of the most common postharvest physiological disorder in horticultural products was detected using hyperspectral imaging and achieved more than 91% detection accuracy in apple, peach, and kiwi fruit [93–96].

4.3. Biochemical Component Analysis

Horticultural crops are rich sources of pigments such as anthocyanin, carotenoid, and chlorophyll, which serve as strong antioxidants and promote human health [31]. Quantification of these pigments has been mainly based on laboratory extraction, which is laborious and time-consuming. Handheld nondestructive devices such as chlorophyll meters and chroma meters were developed as an option to overcome destructive measurement, but they are still limited to be used in large-scale production or breeding programs. Hence, image-based phenotyping of pigment content is receiving increasing attention because it is nondestructive, robust, and fast. Anthocyanin, carotenoid, and chlorophyll content of red lettuce genotypes showed a high correlation with the vegetation indices calculated from images taken by remotely piloted aircraft [31]. The total carotenoid content in cassava root was estimated from the colorimetric indices extracted from the RGB images of root pulp. The total carotenoid content of cassava root showed a high correlation with color indices b^* and chroma [97]. In addition, optical sensors can be used to nondestructively measure the amount of nutrients in the plant, such as nitrogen, phosphorus, and potassium, enabling accurate monitoring of plant growth and precise management of crop production [98].

4.4. Disease Detection and Quantification

Plant diseases are one of the challenges of crop production worldwide, causing significant yield loss every year. Early detection and accurate measurement of disease is a vital part of phytopathology and breeding [10]. Assessment of disease using conventional visual scores and laboratory-based analysis is time-consuming, laborious, and subjective. In recent years, rapid and high-throughput methods for the measurement of disease extent and severity have been widely used based on image analysis captured by various types of sensors [22,48,79,99,100]. High-throughput detection and quantification of disease is especially essential in horticultural crops which are prone to diverse pathogens during pre-harvest and post-harvest handling stages. Image analysis has been widely used for the detection and quantification of horticultural crop diseases such as apple scab [101,102], fire blight [20,21,56,103], powdery mildew [48,104–106], Fusarium wilt [22], bacterial blight [107], bacterial wilt [108], early blight, and late blight [19,99,109–111]. Image analysis can be used to closely monitor the plant health status as the disease infection can be detected at early stages before the development of typical symptoms. This enables us to take appropriate management measures to reduce the yield or quality loss.

4.5. Abiotic Stress Responses

Abiotic stresses are any kind of environmental conditions that affect normal plant growth and yield, such as drought, salinity, heat stress, and cold stress. Rapid and accurate phenotyping of plant responses to various abiotic stresses is essential to accelerate plant breeding programs dealing with the development of climate-resilient genotypes. Image-based high-throughput phenotyping is especially important when screening a large number

of accessions. Various imaging techniques have been used to measure the response of horticultural plants to different abiotic stresses [82,112–114]. Hyperspectral images were used to detect heat stress tolerance in ginseng [115]. Cadmium stress in kale and basil was detected using high-throughput hyperspectral images. Among the vegetation indices analyzed, only the anthocyanin reflectance index was able to detect all levels of cadmium stress in both kale and basil. The anthocyanin reflectance index was significantly higher in cadmium-stressed plants than in the respective controls [116]. The applications of high-throughput phenotyping using image analysis to assess various traits in selected horticultural crops are summarized in Table 3.

Table 3. Applications of image-based high-throughput phenotyping in horticultural crops.

| Crop | Trait | Sensor ^a | Environment | Reference |
|----------------|------------------------------|---------------------|----------------------|-----------------|
| Apple | Seed morphology | RGB | Laboratory | [117] |
| | Plant growth | RGB | Field | [40,118,119] |
| | Fruit detection and counting | RGB | Field | [77,120,121] |
| | Yield prediction | MS, RGB | Field | [45,122] |
| | Fruit ripening | Aerial video | Field | [123] |
| | Winter dormancy | ChlF | Field | [124] |
| | Low oxygen stress | ChlF | Laboratory | [125] |
| | Apple scab | Thermal, MS | Controlled | [101,102] |
| | Fire blight | MS, HS | Field | [21,56,103] |
| | Powdery mildew | RGB, MS | Field | [48] |
| Drought stress | Thermal, MS | Field | [112] | |
| Banana | Plant growth | Laser scanning | Field | [80,126] |
| | Plant counting | MS, laser scanning | Field | [23,126] |
| | Fruit maturity | RGB | Laboratory | [92] |
| | Yellow Sigatoka | RGB | Field | [17] |
| | Multiple diseases | RGB | Field | [49] |
| | Fusarium wilt | MS | Field | [22] |
| Cabbage | Seed morphology | RGB | Laboratory | [127] |
| | Plant growth | RGB | Field | [41] |
| | Shoot biomass | RGB | Field | [33] |
| | Heat stress | MS | Field | [41] |
| Carrot | Root morphology | RGB | Laboratory | [39,128,129] |
| Cassava | Root bulking rate | GPR | Field | [130] |
| | Root morphology | RGB | Field and Laboratory | [131,132] |
| | Shoot biomass | LiDAR | Field | [83] |
| | Root biomass | GPR | Field | [133] |
| | Carotenoid content | RGB | Laboratory | [97] |
| | Starch content | Thermal | Field | [134] |
| | Plant growth | RGB, MS | Controlled and field | [42,135] |
| | Bacterial blight | RGB | Laboratory | [107] |
| Citrus | Plant counting | RGB | Field | [24,81,136,137] |
| | Plant water status | Thermal | Controlled | [54] |
| | Citrus canker | HS | Field | [57] |
| | Huanglongbing (HLB) | GPR, MS, ChlF | Field | [62,138,139] |
| Grape | Bunch architecture | 3D scanner | Field | [140–142] |
| | Berry counting | RGB | Field | [143,144] |
| | Berry maturity | RGB | Laboratory | [145] |
| | Yield prediction | RGB, HS | Field | [47,146–148] |
| | Grape yellows | HS | Field | [79] |
| | Grape leafroll | HS | Laboratory | [149] |
| | Powdery mildew | RGB | Laboratory | [104] |
| | Drought stress | RGB, Thermal | Field | [113] |

Table 3. Cont.

| Crop | Trait | Sensor ^a | Environment | Reference |
|-------------------------|---|---------------------|-------------------|-----------------|
| Lettuce | Seed morphology | RGB | Laboratory | [150] |
| | Leaf semantic components | RGB | Laboratory | [151] |
| | Plant growth | RGB | Controlled | [43,152,153] |
| | Shoot biomass | ChlF | Controlled | [154] |
| | Anthocyanin content | RGB | Field | [31,155] |
| | Carotenoid content | RGB | Field | [31,156] |
| | Chlorophyll content | RGB | Field | [31] |
| | Drought stress | HS, ChlF | Controlled | [63,157,158] |
| | Salt stress | ChlF | Controlled | [64] |
| Mango | Fruit maturity | HS, LiDAR | Field | [159] |
| | Fruit ripening | HS | Field | [60] |
| | Fruit detection | RGB | Field | [30] |
| | Drought stress | Thermal | Field | [78] |
| Pear | Plant growth | RGB | Field | [160] |
| | Fire blight | HS | Field | [20] |
| | Russet | RGB | Laboratory | [50] |
| Pepper | Seed quality | X-ray CT | Laboratory | [161] |
| | Leaf area | RGB | Controlled | [162] |
| Potato | Crop emergence | RGB | Field | [44] |
| | Plant growth | RGB | Controlled | [163] |
| | Tuber growth and development | X-ray CT | Controlled | [164] |
| | Tuber skin color | RGB | Laboratory | [165] |
| | Tuber size | RGB | Laboratory | [166] |
| | Shoot biomass | RGB, HS | Field | [35,167,168] |
| | Nitrogen content | RGB | Field | [169] |
| | Tuber moisture content | HS | Laboratory | [170] |
| | Stomatal conductance | Thermal | Field | [53] |
| | Yield prediction | RGB, Thermal, HS | Field | [46,171] |
| | Early blight | HS | Field | [172] |
| | Late blight | RGB, MS | Field | [19,99,173,174] |
| | Bacterial soft rot | RGB | Laboratory | [51] |
| | Verticillium wilt | MS | Field | [18] |
| | Drought stress | LiDAR | Controlled | [82] |
| | Strawberry | Plant growth | LiDAR | Field |
| Fruit morphology | | RGB | Laboratory | [84,176–178] |
| Shoot biomass | | RGB, Thermal | Field | [28,179,180] |
| Yield prediction | | RGB | Field | [76] |
| Leaf gray mold | | HS | Laboratory | [100] |
| Verticillium wilt | | RGB, MS | Field | [181] |
| Heat and drought stress | | HS | Controlled | [182] |
| Tomato | Root architecture | RGB | Controlled | [38] |
| | Shoot biomass | RGB | Controlled | [29,37] |
| | Fruit morphology | RGB | Laboratory | [183] |
| | Nitrogen, phosphorus, potassium content | MS | Controlled | [98] |
| | Chlorophyll content | RGB, MS | Controlled | [184] |
| | Yield prediction | RGB, MS | Field | [185,186] |
| | Bacterial wilt | ChlF | Controlled | [108,187] |
| | TYLC, early blight, bacterial spot | HS | Field | [16,58] |
| | Drought stress | RGB, Thermal, HS | Controlled, field | [188,189] |
| | Chilling injury (seedling) | ChlF | Controlled | [65] |
| | Salt stress | RGB, MS, Thermal | Field | [36] |

^a Sensor: RGB—red, green, blue; IR—infrared; HS—hyperspectral; MS—multispectral; NIR—near infrared; ChlF—chlorophyll fluorescence; LiDAR—light detection and ranging; GPR—ground penetrating radar.

5. Current Status and Future Perspectives

The statistics of publications related to high-throughput phenotyping in horticultural crops for the last two decades were surveyed and summarized in Figure 3. The number of publications dealing with high-throughput phenotyping using image analysis is increasing every year and is mostly used in agriculture and biological sciences (Figure 3a,b). Among the search keywords, 'fruit' was the most mentioned word in these publications and showed an exponential increase in the last five years (Figure 3c), indicating the increasing interest of the researches to automate the measurement of various fruit traits during growth, maturity, ripening, and postharvest stages. Most of these documents are research articles (71%), followed by review papers (16%) (Figure 3d). Image-based phenotyping studies are actively conducted in many countries, with USA and China taking the lead with more number publications (Figure 3e). The applications of various types of sensors may depend on imaging platforms, accessibility, cost, and the target trait under consideration. Hyperspectral sensors are most popular for the phenotyping of horticultural crops, followed by thermal sensors (Figure 3f).

One of the upcoming challenges in phenomics is the handling of massive amounts of data generated from image-based phenotyping and the ability to extract important knowledge from big data [3]. Here, the application of computer science is inevitable when dealing with digital phenotyping. Specialized in handling multidimensional and multivariate data automatically, it is suitable for application to high-throughput phenotyping [190]. In machine learning (ML), humans are interpretable to the mathematical algorithm models that solve given problems such as classification, regression, and cluster. ML provides prompt results for classifying and identifying the plants or their phenotypes, predicting and estimating the yield or influences of external factors [191].

ML models start by training the dataset. Various algorithms/methods, such as support vector machine (SVM), decision tree, random forest, k-nearest neighbors (KNNs), logistics, regressions, clustering, dimensionality reduction, and artificial neural network (ANN), empower the training. All models require the accumulation of data for their accurate and efficient outputs [192]. Lack of sufficient data learning results in common errors in the output. This issue can be easily fulfilled by massive data processing from image-based high-throughput phenotyping.

However, when the amount of data to be processed is extremely large, deep learning will be more compatible than the other ML algorithms [193,194]. The machine learning applied ANNs is well known as 'deep learning'. Deep learning has similar features but is slightly different from conventional ML types such as supervised learning, unsupervised learning, and reinforcement learning [195]. They differ depending on the absence or presence of human interventions in feature extraction after their training process. Deep learning requires no human intervention if the training data well annotates the targeted feature, while ML requires feature extraction before classification [196]. The most common algorithms used in deep learning are convolutional neural networks (CNN), long short-term memory networks (LSTM network), recurrent neural networks (RNN), multi-layer perceptron (MLP), and radial basis function networks (RBFN).

Despite their differences, both conventional MLs and deep learning provide powerful results. Therefore, appropriate selection based on the purpose and limitations would provide more advantages during the process. For instance, ML is generally used in the evaluation and prediction of stress, biomasses, and yields [16,28,171,173,186]. Deep learning is more proper in the detection, recognition, and counting of objects in large and complex datasets such as biotic/abiotic stresses and individual plants [197,198]. Recently, ML and DL methods have been increasingly used in high-throughput plant phenotyping of various traits (Table 4).

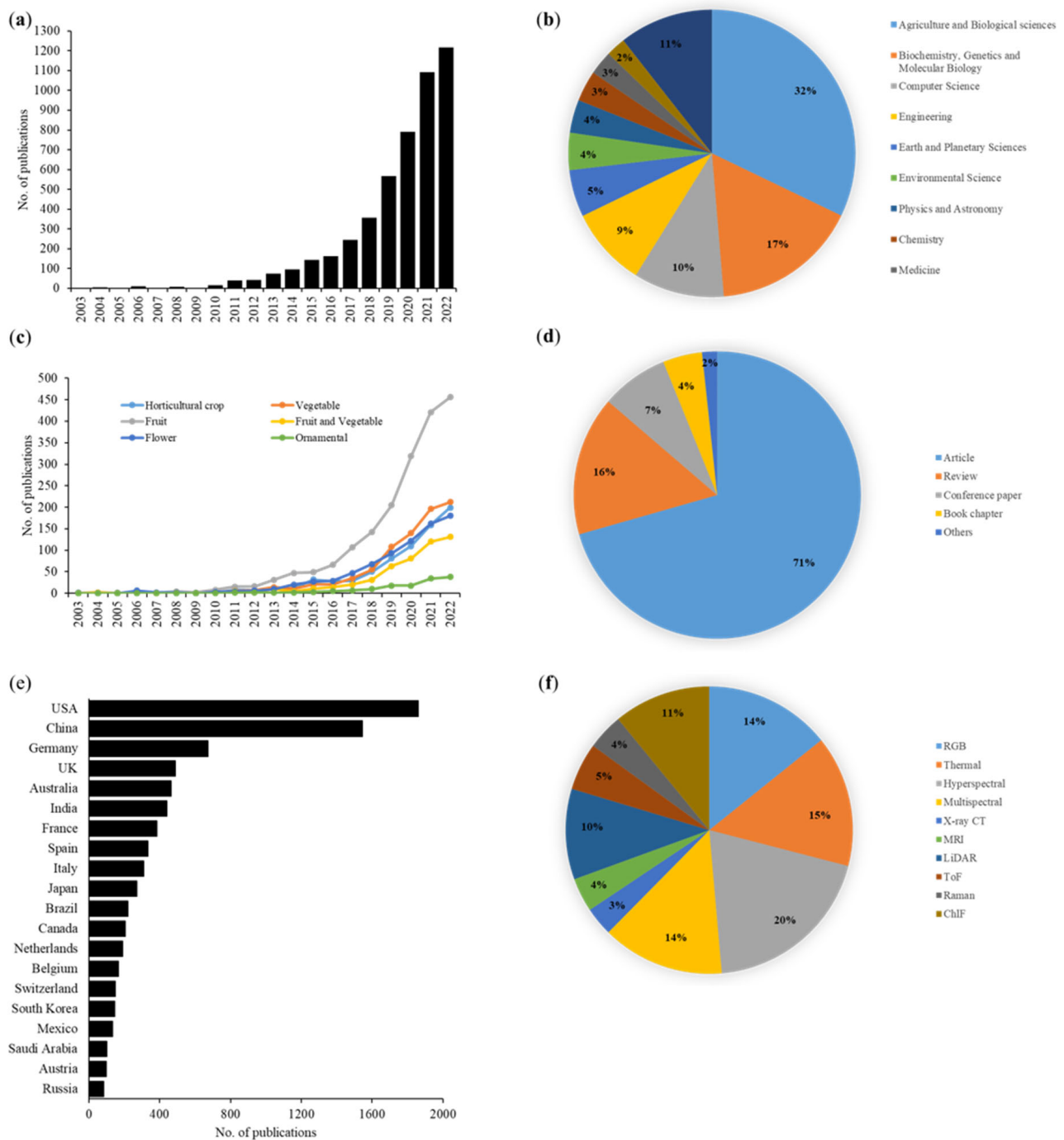


Figure 3. Statistics of image-based high-throughput phenotyping studies in horticultural crops during the past two decades. (a) The number of annual publications related to image-based phenotyping of horticultural crops. (b) Major areas of research using image-based high-throughput phenotyping. (c) Annual number of publications with different search keywords. (d) The type of publications related to image-based high-throughput phenotyping of horticultural crops. (e) Number of image-based high-throughput phenotyping studies by country (top 20). (f) Type of imaging techniques for high-throughput phenotyping of horticultural crops. Note: the data were obtained from the Scopus (<https://www.scopus.com>) database (Elsevier, The Netherlands) accessed on 21 February 2023. The publications were searched using keywords: horticultural crop, fruit, vegetable, ornamental, flower, and sensor types (RGB, thermal, hyperspectral, multispectral, X-ray CT, MRI, LiDAR, ToF, Raman, ChIF) within the search results of high-throughput phenotyping using image analysis.

Table 4. Examples of machine learning and deep learning applications in high-throughput plant phenotyping.

| Algorithm Application | Algorithm Type | Imaging Technique | Plant Species | Phenotypic Trait | Reference |
|-----------------------|---|-------------------|---------------|------------------------------|-----------|
| Classification | Faster R-CNN | RGB | Strawberry | Yield prediction | [76] |
| Classification | Convolution Network | X-ray CT | Watermelon | Seed quality | [70] |
| Classification | Linear Discriminance Model, Partially Least Square, Multi-Layer Perceptron, Radial-Basis Function Network | Hyperspectral | Grape | Grape yellows | [79] |
| Classification | YOLOv3 | Multispectral | Hamlin citrus | Plant counting | [81] |
| Detection | 3D Point clouds | Visible light | Apple | Fruit detection and counting | [77] |
| Detection | Convolutional Neural Network, Template Matching, Local Maximum Filter | Thermal | Banana | Plant counting | [23] |
| Identification | Neural Network Radial Basis Function, K-Nearest Neighbor | Hyperspectral | Tomato | bacterial spot | [58] |
| Identification | PCA | Fluorescence | Letucce | Salt stress | [64] |
| Identification | EVI2 Threshold | Multispectral | Banana | Plant growth | [80] |
| Identification | Logistic Regression | LiDAR | Potato | Drought stress | [82] |

Available aerial high-throughput phenotyping platforms target the measurement of above-ground parts, while field-scale root phenotyping using images remains a bottleneck. Novel technologies enabling root phenotyping at the field level will be a breakthrough, especially for root and tuber crops, to capture root system architecture and to predict the yield of these underground parts at the field level. With the development of novel technologies with respect to sensing and data analysis methods, image-based phenotyping can discover new traits which were difficult to measure or detect using conventional phenotyping [3]. The newly discovered traits, in combination with the available omics data, need to be explored for the new frontier of crop improvement. The storage and sharing of the large amount of phenomic data obtained from image-based phenotyping are still challenging and need to be resolved. The data should be standardized and easily accessible among research communities, academia, industry, and farmers. Minimizing the cost of sensors and phenotyping platforms, along with the automation of big data analysis methods, will greatly increase the significance of phenomics in crop improvement to meet the projected global food demand.

6. Conclusions

Image-based phenotyping methods have become an integral part of plant breeding, cultivation, and quality assessment of economically important crops. This review highlights the progress and applications of image-based phenotyping as applied to horticultural crops. We explored commonly used imaging techniques: RGB, thermal, hyperspectral, fluorescence, and tomographic imaging with their advantages and drawbacks in relation to high-throughput phenotyping of horticultural crop traits. They are used to measure morphological, physiological, biochemical, disease and pest, and abiotic stresses.

In addition to accelerating the breeding cycle by enabling rapid and accurate measurement of phenotypic traits in a large population, image-based phenotyping will help to monitor the plant condition and make immediate decisions such as pesticide spray, fertilization, or harvesting, which will greatly improve yield and the quality of the produce. Moreover, the physiological processes of horticultural crops continue even after harvest, and their quality is highly dependent on postharvest storage and handling conditions. Hence, image-based phenotyping is especially important for postharvest phenotyping of horticultural crops. This will allow real-time monitoring of internal and external qualities of

the horticultural product and will continue to play a significant role along the horticultural chain. Machine learning and deep learning technologies should be well integrated into image-based phenotyping to mine knowledge from the massive amount of data generated.

Author Contributions: A.M.A. wrote the original draft, Y.K. and J.K. contributed to writing the machine learning and deep learning section, S.L.K. advised on the contents of the manuscript, and J.B. reviewed and edited the manuscript. All authors have read and agreed to the published version of the manuscript.

Funding: This work was carried out with the support of the “Cooperative Research Program for Agriculture Science and Technology Development (Project No. PJ01673501)”, Rural Development Administration, Republic of Korea.

Institutional Review Board Statement: Not applicable.

Informed Consent Statement: Not applicable.

Data Availability Statement: Not applicable.

Conflicts of Interest: The authors declare no conflict of interest.

References

- Hickey, L.T.; Hafeez, A.N.; Robinson, H.; Jackson, S.A.; Leal-Bertioli, S.C.M.; Tester, M.; Gao, C.; Godwin, I.D.; Hayes, B.J.; Wulff, B.B.H. Breeding crops to feed 10 billion. *Nat. Biotechnol.* **2019**, *37*, 744–754. [[CrossRef](#)]
- Yang, W.; Feng, H.; Zhang, X.; Zhang, J.; Doonan, J.H.; Batchelor, W.D.; Xiong, L.; Yan, J. Crop Phenomics and High-Throughput Phenotyping: Past Decades, Current Challenges, and Future Perspectives. *Mol. Plant* **2020**, *13*, 187–214. [[CrossRef](#)]
- Sun, D.; Robbins, K.; Morales, N.; Shu, Q.; Cen, H. Advances in optical phenotyping of cereal crops. *Trends Plant Sci.* **2022**, *27*, 191–208. [[CrossRef](#)]
- Werner, T. Next generation sequencing in functional genomics. *Brief. Bioinform.* **2010**, *11*, 499–511. [[CrossRef](#)]
- Fasoula, D.A.; Ioannides, I.M.; Omirou, M. Phenotyping and Plant Breeding: Overcoming the Barriers. *Front. Plant Sci.* **2020**, *10*, 1713. [[CrossRef](#)]
- Li, D.; Quan, C.; Song, Z.; Li, X.; Yu, G.; Li, C.; Muhammad, A. High-Throughput Plant Phenotyping Platform (HT3P) as a Novel Tool for Estimating Agronomic Traits From the Lab to the Field. *Front. Bioeng. Biotechnol.* **2021**, *8*, 623705. [[CrossRef](#)]
- Das Choudhury, S.; Samal, A.; Awada, T. Leveraging Image Analysis for High-Throughput Plant Phenotyping. *Front. Plant Sci.* **2019**, *10*, 508. [[CrossRef](#)]
- Chawade, A.; van Ham, J.; Blomquist, H.; Bagge, O.; Alexandersson, E.; Ortiz, R. High-Throughput Field-Phenotyping Tools for Plant Breeding and Precision Agriculture. *Agronomy* **2019**, *9*, 258. [[CrossRef](#)]
- Jangra, S.; Chaudhary, V.; Yadav, R.C.; Yadav, N.R. High-Throughput Phenotyping: A Platform to Accelerate Crop Improvement. *Phenomics* **2021**, *1*, 31–53. [[CrossRef](#)]
- Mutka, A.M.; Bart, R.S. Image-based phenotyping of plant disease symptoms. *Front. Plant Sci.* **2015**, *5*, 734. [[CrossRef](#)]
- Li, L.; Zhang, Q.; Huang, D. A review of imaging techniques for plant phenotyping. *Sensors* **2014**, *14*, 20078–20111. [[CrossRef](#)]
- He, F.; Meng, Q.; Tang, L.; Huang, X.; Lu, X.; Wang, R.; Zhang, K.; Li, Y. Research progress in hyperspectral imaging technology for fruit quality detection. *J. Fruit Sci.* **2021**, *38*, 1590–1599.
- Haque, S.; Lobaton, E.; Nelson, N.; Yencho, G.C.; Pecota, K.V.; Mierop, R.; Kudenov, M.W.; Boyette, M.; Williams, C.M. Computer vision approach to characterize size and shape phenotypes of horticultural crops using high-throughput imagery. *Comput. Electron. Agric.* **2021**, *182*, 106011. [[CrossRef](#)]
- Lu, Y.; Saeys, W.; Kim, M.; Peng, Y.; Lu, R. Hyperspectral imaging technology for quality and safety evaluation of horticultural products: A review and celebration of the past 20-year progress. *Postharvest. Biol. Technol.* **2020**, *170*, 111318. [[CrossRef](#)]
- Du, J.; Fan, J.; Wang, C.; Lu, X.; Zhang, Y.; Wen, W.; Liao, S.; Yang, X.; Guo, X.; Zhao, C. Greenhouse-based vegetable high-throughput phenotyping platform and trait evaluation for large-scale lettuces. *Comput. Electron. Agric.* **2021**, *186*, 106193. [[CrossRef](#)]
- Abdulridha, J.; Ampatzidis, Y.; Qureshi, J.; Roberts, P. Laboratory and UAV-based identification and classification of tomato yellow leaf curl, bacterial spot, and target spot diseases in tomato utilizing hyperspectral imaging and machine learning. *Remote Sens.* **2020**, *12*, 2732. [[CrossRef](#)]
- Calou, V.B.C.; Teixeira, A.D.S.; Moreira, L.C.J.; Lima, C.S.; de Oliveira, J.B.; de Oliveira, M.R.R. The use of UAVs in monitoring yellow sigatoka in banana. *Biosyst. Eng.* **2020**, *193*, 115–125. [[CrossRef](#)]
- Lizarazo, I.; Rodriguez, J.L.; Cristancho, O.; Olaya, F.; Duarte, M.; Prieto, F. Identification of symptoms related to potato Verticillium wilt from UAV-based multispectral imagery using an ensemble of gradient boosting machines. *Smart Agric. Technol.* **2023**, *3*, 100138. [[CrossRef](#)]
- Rodríguez, J.; Lizarazo, I.; Prieto, F.; Angulo-Morales, V. Assessment of potato late blight from UAV-based multispectral imagery. *Comput. Electron. Agric.* **2021**, *184*, 106061. [[CrossRef](#)]

20. Schoofs, H.; Delalieux, S.; Deckers, T.; Bylemans, D. Fire blight monitoring in pear orchards by unmanned airborne vehicles (UAV) systems carrying spectral sensors. *Agronomy* **2020**, *10*, 615. [[CrossRef](#)]
21. Xiao, D.; Pan, Y.; Feng, J.; Yin, J.; Liu, Y.; He, L. Remote sensing detection algorithm for apple fire blight based on UAV multispectral image. *Comput. Electron. Agric.* **2022**, *199*, 107137. [[CrossRef](#)]
22. Zhang, S.; Li, X.; Ba, Y.; Lyu, X.; Zhang, M.; Li, M. Banana Fusarium Wilt Disease Detection by Supervised and Unsupervised Methods from UAV-Based Multispectral Imagery. *Remote Sens.* **2022**, *14*, 1231. [[CrossRef](#)]
23. Aeberli, A.; Johansen, K.; Robson, A.; Lamb, D.W.; Phinn, S. Detection of banana plants using multi-temporal multispectral UAV imagery. *Remote Sens.* **2021**, *13*, 2123. [[CrossRef](#)]
24. Donmez, C.; Villi, O.; Berberoglu, S.; Cilek, A. Computer vision-based citrus tree detection in a cultivated environment using UAV imagery. *Comput. Electron. Agric.* **2021**, *187*, 106273. [[CrossRef](#)]
25. Osco, L.P.; Nogueira, K.; Marques Ramos, A.P.; Faita Pinheiro, M.M.; Furuya, D.E.G.; Gonçalves, W.N.; de Castro Jorge, L.A.; Marcato Junior, J.; dos Santos, J.A. Semantic segmentation of citrus-orchard using deep neural networks and multispectral UAV-based imagery. *Precis. Agric.* **2021**, *22*, 1171–1188. [[CrossRef](#)]
26. Ballesteros, R.; Ortega, J.F.; Hernandez, D.; Moreno, M.A. Onion biomass monitoring using UAV-based RGB imaging. *Precis. Agric.* **2018**, *19*, 840–857. [[CrossRef](#)]
27. Liu, Y.; Feng, H.; Yue, J.; Fan, Y.; Jin, X.; Zhao, Y.; Song, X.; Long, H.; Yang, G. Estimation of Potato Above-Ground Biomass Using UAV-Based Hyperspectral Images and Machine-Learning Regression. *Remote Sens.* **2022**, *14*, 5449. [[CrossRef](#)]
28. Zheng, C.; Abd-Elrahman, A.; Whitaker, V.; Dalid, C. Prediction of Strawberry Dry Biomass from UAV Multispectral Imagery Using Multiple Machine Learning Methods. *Remote Sens.* **2022**, *14*, 4511. [[CrossRef](#)]
29. Johansen, K.; Morton, M.J.L.; Malbeteau, Y.; Aragon, B.; Al-Mashharawi, S.; Ziliani, M.G.; Angel, Y.; Fiene, G.; Negrão, S.; Mousa, M.A.A.; et al. Predicting Biomass and Yield in a Tomato Phenotyping Experiment Using UAV Imagery and Random Forest. *Front. Artif. Intell.* **2020**, *3*, 28. [[CrossRef](#)]
30. Xiong, J.; Liu, Z.; Chen, S.; Liu, B.; Zheng, Z.; Zhong, Z.; Yang, Z.; Peng, H. Visual detection of green mangoes by an unmanned aerial vehicle in orchards based on a deep learning method. *Biosyst. Eng.* **2020**, *194*, 261–272. [[CrossRef](#)]
31. Clemente, A.A.; Maciel, G.M.; Siquieroli, A.C.S.; Gallis, R.B.D.A.; Pereira, L.M.; Duarte, J.G. High-throughput phenotyping to detect anthocyanins, chlorophylls, and carotenoids in red lettuce germplasm. *Int. J. Appl. Earth Obs. Geoinf.* **2021**, *103*, 102533. [[CrossRef](#)]
32. Kim, J.; Chung, Y.S. A short review of RGB sensor applications for accessible high-throughput phenotyping. *J. Crop Sci. Biotechnol.* **2021**, *24*, 495–499. [[CrossRef](#)]
33. Sinde-González, I.; Gómez-López, J.P.; Tapia-Navarro, S.A.; Murgueitio, E.; Falconí, C.; Benítez, F.L.; Toulkeridis, T. Determining the Effects of Nanonutrient Application in Cabbage (*Brassica oleracea* var. *capitata* L.) Using Spectrometry and Biomass Estimation with UAV. *Agronomy* **2022**, *12*, 81. [[CrossRef](#)]
34. Li, B.; Xu, X.; Zhang, L.; Han, J.; Bian, C.; Li, G.; Liu, J.; Jin, L. Above-ground biomass estimation and yield prediction in potato by using UAV-based RGB and hyperspectral imaging. *ISPRS J. Photogramm. Remote Sens.* **2020**, *162*, 161–172. [[CrossRef](#)]
35. Liu, Y.; Feng, H.; Yue, J.; Jin, X.; Li, Z.; Yang, G. Estimation of potato above-ground biomass based on unmanned aerial vehicle red-green-blue images with different texture features and crop height. *Front. Plant Sci.* **2022**, *13*, 938216. [[CrossRef](#)]
36. Johansen, K.; Morton, M.J.L.; Malbeteau, Y.M.; Aragon, B.; Al-Mashharawi, S.K.; Ziliani, M.G.; Angel, Y.; Fiene, G.M.; Negrão, S.S.C.; Mousa, M.A.A.; et al. Unmanned aerial vehicle-based phenotyping using morphometric and spectral analysis can quantify responses of wild tomato plants to salinity stress. *Front. Plant Sci.* **2019**, *10*, 370. [[CrossRef](#)]
37. Laxman, R.H.; Hemamalini, P.; Bhatt, R.M.; Sadashiva, A.T. Non-invasive quantification of tomato (*Solanum lycopersicum* L.) plant biomass through digital imaging using phenomics platform. *Indian J. Plant Physiol.* **2018**, *23*, 369–375. [[CrossRef](#)]
38. Alaguero-Cordovilla, A.; Gran-Gómez, F.J.; Tormos-Moltó, S.; Pérez-Pérez, J.M. Morphological characterization of root system architecture in diverse tomato genotypes during early growth. *Int. J. Mol. Sci.* **2018**, *19*, 3888. [[CrossRef](#)]
39. Brainard, S.H.; Bustamante, J.A.; Dawson, J.C.; Spalding, E.P.; Goldman, I.L. A Digital Image-Based Phenotyping Platform for Analyzing Root Shape Attributes in Carrot. *Front. Plant Sci.* **2021**, *12*, 690031. [[CrossRef](#)]
40. Hobart, M.; Pflanz, M.; Weltzien, C.; Schirrmann, M. Growth height determination of tree walls for precise monitoring in apple fruit production using UAV photogrammetry. *Remote Sens.* **2020**, *12*, 1656. [[CrossRef](#)]
41. Kim, D.W.; Yun, H.S.; Jeong, S.J.; Kwon, Y.S.; Kim, S.G.; Lee, W.S.; Kim, H.J. Modeling and testing of growth status for Chinese cabbage and white radish with UAV-based RGB imagery. *Remote Sens.* **2018**, *10*, 563. [[CrossRef](#)]
42. Wasonga, D.O.; Yaw, A.; Kleemola, J.; Alakukku, L.; Mäkelä, P.S.A. Red-green-blue and multispectral imaging as potential tools for estimating growth and nutritional performance of cassava under deficit irrigation and potassium fertilization. *Remote Sens.* **2021**, *13*, 598. [[CrossRef](#)]
43. Gang, M.S.; Kim, H.J.; Kim, D.W. Estimation of Greenhouse Lettuce Growth Indices Based on a Two-Stage CNN Using RGB-D Images. *Sensors* **2022**, *22*, 5499. [[CrossRef](#)] [[PubMed](#)]
44. Li, B.; Xu, X.; Han, J.; Zhang, L.; Bian, C.; Jin, L.; Liu, J. The estimation of crop emergence in potatoes by UAV RGB imagery. *Plant Methods* **2019**, *15*, 15. [[CrossRef](#)] [[PubMed](#)]
45. Chen, R.; Zhang, C.; Xu, B.; Zhu, Y.; Zhao, F.; Han, S.; Yang, G.; Yang, H. Predicting individual apple tree yield using UAV multi-source remote sensing data and ensemble learning. *Comput. Electron. Agric.* **2022**, *201*, 107275. [[CrossRef](#)]

46. Elsayed, S.; El-Hendawy, S.; Khadr, M.; Elsherbiny, O.; Al-Suhaibani, N.; Alotaibi, M.; Tahir, M.U.; Darwish, W. Combining thermal and RGB imaging indices with multivariate and data-driven modeling to estimate the growth, water status, and yield of potato under different drip irrigation regimes. *Remote Sens.* **2021**, *13*, 1679. [[CrossRef](#)]
47. Kurtser, P.; Ringdahl, O.; Rotstein, N.; Berenstein, R.; Edan, Y. In-field grape cluster size assessment for vine yield estimation using a mobile robot and a consumer level RGB-D Camera. *IEEE Robot. Autom. Lett.* **2020**, *5*, 2031–2038. [[CrossRef](#)]
48. Chandel, A.K.; Khot, L.R.; Sallato, B. Apple powdery mildew infestation detection and mapping using high-resolution visible and multispectral aerial imaging technique. *Sci. Hortic.* **2021**, *287*, 110228. [[CrossRef](#)]
49. Gomez Selvaraj, M.; Vergara, A.; Montenegro, F.; Alonso Ruiz, H.; Safari, N.; Raymaekers, D.; Ocimati, W.; Ntamwira, J.; Tits, L.; Omondi, A.B.; et al. Detection of banana plants and their major diseases through aerial images and machine learning methods: A case study in DR Congo and Republic of Benin. *ISPRS J. Photogramm. Remote Sens.* **2020**, *169*, 110–124. [[CrossRef](#)]
50. Kim, Y.; Oh, S.; Kim, K.; Jeong, H.W.; Kim, D. Bi-dimensional Image Analysis for the Phenotypic Evaluation of Russet in Asian Pear (*Pyrus* spp.). *Hortic. Sci. Technol.* **2022**, *40*, 192–198.
51. Lee, U.; Silva, R.R.; Kim, C.; Kim, H.; Heo, S.; Park, I.S.; Kim, W.; Jansky, S.; Chung, Y.S. Image Analysis for Measuring Disease Symptom to Bacterial Soft Rot in Potato. *Am. J. Potato Res.* **2019**, *90*, 303–313. [[CrossRef](#)]
52. Ahmadi, S.H.; Agharezaee, M.; Kamgar-Haghighi, A.A.; Sepaskhah, A.R. Comparing canopy temperature and leaf water potential as irrigation scheduling criteria of potato in water-saving irrigation strategies. *Int. J. Plant Prod.* **2017**, *11*, 333–348.
53. Prashar, A.; Yildiz, J.; McNicol, J.W.; Bryan, G.J.; Jones, H.G. Infra-red Thermography for High Throughput Field Phenotyping in *Solanum tuberosum*. *PLoS ONE* **2013**, *8*, e65816. [[CrossRef](#)] [[PubMed](#)]
54. Vieira, G.H.S.; Ferrarezi, R.S. Use of thermal imaging to assess water status in citrus plants in greenhouses. *Horticulturae* **2021**, *7*, 249. [[CrossRef](#)]
55. Sarić, R.; Nguyen, V.D.; Burge, T.; Berkowitz, O.; Trtílek, M.; Whelan, J.; Lewsey, M.G.; Čustović, E. Applications of hyperspectral imaging in plant phenotyping. *Trends Plant Sci.* **2022**, *27*, 301–315. [[CrossRef](#)]
56. Skoneczny, H.; Kubiak, K.; Spiralski, M.; Kotlarz, J. Fire blight disease detection for apple trees: Hyperspectral analysis of healthy, infected and dry leaves. *Remote Sens.* **2020**, *12*, 2101. [[CrossRef](#)]
57. Abdulridha, J.; Batuman, O.; Ampatzidis, Y. UAV-based remote sensing technique to detect citrus canker disease utilizing hyperspectral imaging and machine learning. *Remote Sens.* **2019**, *11*, 1373. [[CrossRef](#)]
58. Abdulridha, J.; Ampatzidis, Y.; Kakarla, S.C.; Roberts, P. Detection of target spot and bacterial spot diseases in tomato using UAV-based and benchtop-based hyperspectral imaging techniques. *Precis. Agric.* **2020**, *21*, 955–978. [[CrossRef](#)]
59. Shao, Y.; Wang, Y.; Xuan, G.; Gao, Z.; Hu, Z.; Gao, C.; Wang, K. Assessment of Strawberry Ripeness Using Hyperspectral Imaging. *Anal. Lett.* **2020**, *54*, 1547–1560. [[CrossRef](#)]
60. Gutiérrez, S.; Wendel, A.; Underwood, J. Spectral filter design based on in-field hyperspectral imaging and machine learning for mango ripeness estimation. *Comput. Electron. Agric.* **2019**, *164*, 104890. [[CrossRef](#)]
61. Maxwell, K.; Johnson, G.N. Chlorophyll fluorescence—A practical guide. *J. Exp. Bot.* **2000**, *51*, 659–668. [[CrossRef](#)] [[PubMed](#)]
62. Weng, H.Y.; Zeng, Y.B.; Cen, H.Y.; He, M.B.; Meng, Y.Q.; Liu, Y.; Wan, L.; Xu, H.X.; Li, H.Y.; Fang, H.; et al. Characterization and detection of leaf photosynthetic response to citrus huanglongbing from cool to hot seasons in two orchards. *Trans. ASABE* **2020**, *63*, 501–512. [[CrossRef](#)]
63. Kumar, P.; Eriksen, R.L.; Simko, I.; Mou, B. Molecular Mapping of Water-Stress Responsive Genomic Loci in Lettuce (*Lactuca* spp.) Using Kinetics Chlorophyll Fluorescence, Hyperspectral Imaging and Machine Learning. *Front. Genet.* **2021**, *12*, 634554. [[CrossRef](#)] [[PubMed](#)]
64. Adhikari, N.D.; Simko, I.; Mou, B. Phenomic and physiological analysis of salinity effects on lettuce. *Sensors* **2019**, *19*, 4814. [[CrossRef](#)] [[PubMed](#)]
65. Dong, Z.; Men, Y.; Li, Z.; Zou, Q.; Ji, J. Chlorophyll fluorescence imaging as a tool for analyzing the effects of chilling injury on tomato seedlings. *Sci. Hortic.* **2019**, *246*, 490–497. [[CrossRef](#)]
66. Metzner, R.; Eggert, A.; van Dusschoten, D.; Pflugfelder, D.; Gerth, S.; Schurr, U.; Uhlmann, N.; Jahnke, S. Direct comparison of MRI and X-ray CT technologies for 3D imaging of root systems in soil: Potential and challenges for root trait quantification. *Plant Methods* **2015**, *11*, 17. [[CrossRef](#)]
67. Borisjuk, L.; Rolletschek, H.; Neuberger, T. Surveying the plant's world by magnetic resonance imaging. *Plant J.* **2012**, *70*, 129–146. [[CrossRef](#)]
68. Piovesan, A.; Vancauwenberghe, V.; Van De Looverbosch, T.; Verboven, P.; Nicolai, B. X-ray computed tomography for 3D plant imaging. *Trends Plant Sci.* **2021**, *26*, 1171–1185. [[CrossRef](#)]
69. Liu, W.; Liu, C.; Jin, J.; Li, D.; Fu, Y.; Yuan, X. High-Throughput Phenotyping of Morphological Seed and Fruit Characteristics Using X-Ray Computed Tomography. *Front. Plant Sci.* **2020**, *11*, 601475. [[CrossRef](#)]
70. Ahmed, M.R.; Yasmin, J.; Park, E.; Kim, G.; Kim, M.S.; Wakholi, C.; Mo, C.; Cho, B.K. Classification of watermelon seeds using morphological patterns of x-ray imaging: A comparison of conventional machine learning and deep learning. *Sensors* **2020**, *20*, 6753. [[CrossRef](#)]
71. Agostini, A.; Alenyà, G.; Fischbach, A.; Scharr, H.; Wörgötter, F.; Torras, C. A cognitive architecture for automatic gardening. *Comput. Electron. Agric.* **2017**, *138*, 69–79. [[CrossRef](#)]
72. Kim, D.M.; Zhang, H.; Zhou, H.; Du, T.; Wu, Q.; Mockler, T.C.; Berezin, M.Y. Highly sensitive image-derived indices of water-stressed plants using hyperspectral imaging in SWIR and histogram analysis. *Sci. Rep.* **2015**, *5*, 15919. [[CrossRef](#)] [[PubMed](#)]

73. Blonder, B.; De Carlo, F.; Moore, J.; Rivers, M.; Enquist, B.J. X-ray imaging of leaf venation networks. *N. Phytol.* **2012**, *196*, 1274–1282. [[CrossRef](#)] [[PubMed](#)]
74. Kim, J.Y. Roadmap to High Throughput Phenotyping for Plant Breeding. *J. Biosyst. Eng.* **2020**, *45*, 43–55. [[CrossRef](#)]
75. Bian, L.; Zhang, H.; Ge, Y.; Čepl, J.; Stejskal, J.; El-Kassaby, Y.A. Closing the gap between phenotyping and genotyping: Review of advanced, image-based phenotyping technologies in forestry. *Ann. For. Sci.* **2022**, *79*, 22. [[CrossRef](#)]
76. Chen, Y.; Lee, W.S.; Gan, H.; Peres, N.; Fraisse, C.; Zhang, Y.; He, Y. Strawberry yield prediction based on a deep neural network using high-resolution aerial orthoimages. *Remote Sens.* **2019**, *11*, 1584. [[CrossRef](#)]
77. Zine-El-Abidine, M.; Dutagaci, H.; Galopin, G.; Rousseau, D. Assigning apples to individual trees in dense orchards using 3D colour point clouds. *Biosyst. Eng.* **2021**, *209*, 30–52. [[CrossRef](#)]
78. Taria, S.; Alam, B.; Rane, J.; Kumar, M.; Babar, R.; Singh, N.P. Deciphering endurance capacity of mango tree (*Mangifera indica* L.) to desiccation stress using modern physiological tools. *Sci. Hortic.* **2022**, *303*, 111247. [[CrossRef](#)]
79. Bendel, N.; Backhaus, A.; Kicherer, A.; Köckerling, J.; Maixner, M.; Jarausch, B.; Biancu, S.; Klück, H.C.; Seiffert, U.; Voegelé, R.T.; et al. Detection of two different grapevine yellows in *Vitis vinifera* using hyperspectral imaging. *Remote Sens.* **2020**, *12*, 4151. [[CrossRef](#)]
80. Aeberli, A.; Phinn, S.; Johansen, K.; Robson, A.; Lamb, D.W. Characterisation of Banana Plant Growth Using High-Spatiotemporal-Resolution Multispectral UAV Imagery. *Remote Sens.* **2023**, *15*, 679. [[CrossRef](#)]
81. Ampatzidis, Y.; Partel, V. UAV-based high throughput phenotyping in citrus utilizing multispectral imaging and artificial intelligence. *Remote Sens.* **2019**, *11*, 410. [[CrossRef](#)]
82. Mulugeta Aneley, G.; Haas, M.; Köhl, K. LIDAR-Based Phenotyping for Drought Response and Drought Tolerance in Potato. *Potato Res.* **2022**. [[CrossRef](#)]
83. Adams, T.; Bruton, R.; Ruiz, H.; Barrios-Perez, I.; Selvaraj, M.G.; Hays, D.B. Prediction of aboveground biomass of three cassava (*Manihot esculenta*) genotypes using a terrestrial laser scanner. *Remote Sens.* **2021**, *13*, 1272. [[CrossRef](#)]
84. Nagamatsu, S.; Tsubone, M.; Wada, T.; Oku, K.; Mori, M.; Hirata, C.; Hayashi, A.; Tanabata, T.; Isobe, S.; Takata, K.; et al. Strawberry fruit shape: Quantification by image analysis and qtl detection by genome-wide association analysis. *Breed Sci.* **2021**, *71*, 167–175. [[CrossRef](#)]
85. Alfatni, M.S.M.; Shariff, A.R.M.; Shafri, H.Z.M.; Saaed, O.M.B.; Eshanta, O.M. Oil palm fruit bunch grading system using red, green and blue digital number. *J. Appl. Sci.* **2008**, *8*, 1444–1452. [[CrossRef](#)]
86. Rifna, E.J.; Dwivedi, M. Emerging nondestructive technologies for quality assessment of fruits, vegetables, and cereals. In *Food Losses, Sustainable Postharvest and Food Technologies*, 1st ed.; Galanakis, C.M., Ed.; Elsevier: Amsterdam, The Netherlands, 2021; pp. 219–253.
87. Subhashree, S.N.; Sunoj, S.; Xue, J.; Bora, G.C. Quantification of browning in apples using colour and textural features by image analysis. *Food Qual. Saf.* **2017**, *1*, 221–226. [[CrossRef](#)]
88. OIV. *OIV Descriptor List for Grape Varieties and Vitis Species*, 2nd ed.; International Organisation of Vine and Wine: Paris, France, 2009.
89. Underhill, A.N.; Hirsch, C.D.; Clark, M.D. Evaluating and Mapping Grape Color Using Image-Based Phenotyping. *Plant Phenomics* **2020**, *2020*, 8086309. [[CrossRef](#)]
90. Kuhl, F.P.; Giardina, C.R. Elliptical Fourier features of a closed contour. *Comput. Electron. Agric.* **1982**, *18*, 236–258. [[CrossRef](#)]
91. Kaur, H.; Sawhney, B.K.; Jawandha, S.K. Evaluation of plum fruit maturity by image processing techniques. *J. Food Sci. Technol.* **2018**, *55*, 3008–3015. [[CrossRef](#)]
92. Surya Prabha, D.; Sathesh Kumar, J. Assessment of banana fruit maturity by image processing technique. *J. Food Sci. Technol.* **2015**, *52*, 1316–1327. [[CrossRef](#)]
93. ElMasry, G.; Wang, N.; Vigneault, C. Detecting chilling injury in Red Delicious apple using hyperspectral imaging and neural networks. *Postharvest Biol. Technol.* **2009**, *52*, 1–8. [[CrossRef](#)]
94. Pan, L.; Zhang, Q.; Zhang, W.; Sun, Y.; Hu, P.; Tu, K. Detection of cold injury in peaches by hyperspectral reflectance imaging and artificial neural network. *Food Chem.* **2016**, *192*, 134–141. [[CrossRef](#)] [[PubMed](#)]
95. Ge, Y.; Tu, S. Identification of Chilling Injury in Kiwifruit Using Hyperspectral Structured-Illumination Reflectance Imaging System (SIRI) with Support Vector Machine (SVM) Modelling. *Anal. Lett.* **2022**, *56*, 2040–2052. [[CrossRef](#)]
96. Lu, Y.; Lu, R. Detection of chilling injury in pickling cucumbers using dual-band chlorophyll fluorescence imaging. *Foods* **2021**, *10*, 1094. [[CrossRef](#)] [[PubMed](#)]
97. De Carvalho, R.R.B.; Cortes, D.F.M.; e Sousa, M.B.; de Oliveira, L.A.; de Oliveira, E.J. Image-based phenotyping of cassava roots for diversity studies and carotenoids prediction. *PLoS ONE* **2022**, *17*, e0263326. [[CrossRef](#)] [[PubMed](#)]
98. Sun, G.; Ding, Y.; Wang, X.; Lu, W.; Sun, Y.; Yu, H. Nondestructive determination of nitrogen, phosphorus and potassium contents in greenhouse tomato plants based on multispectral three-dimensional imaging. *Sensors* **2019**, *19*, 5295. [[CrossRef](#)]
99. Sugiura, R.; Tsuda, S.; Tamiya, S.; Itoh, A.; Nishiwaki, K.; Murakami, N.; Shibuya, Y.; Hirafuji, M.; Nuske, S. Field phenotyping system for the assessment of potato late blight resistance using RGB imagery from an unmanned aerial vehicle. *Biosyst. Eng.* **2016**, *148*, 1–10. [[CrossRef](#)]
100. Wu, G.; Fang, Y.; Jiang, Q.; Cui, M.; Li, N.; Ou, Y.; Diao, Z.; Zhang, B. Early identification of strawberry leaves disease utilizing hyperspectral imaging combing with spectral features, multiple vegetation indices and textural features. *Comput. Electron. Agric.* **2023**, *204*, 107553. [[CrossRef](#)]

101. Belin, É.; Rousseau, D.; Boureau, T.; Caffier, V. Thermography versus chlorophyll fluorescence imaging for detection and quantification of apple scab. *Comput. Electron. Agric.* **2013**, *90*, 159–163. [[CrossRef](#)]
102. Bleasdale, A.J.; Blackburn, G.A.; Whyatt, J.D. Feasibility of detecting apple scab infections using low-cost sensors and interpreting radiation interactions with scab lesions. *Int. J. Remote Sens.* **2022**, *43*, 4984–5005. [[CrossRef](#)]
103. Jarolmasjed, S.; Sankaran, S.; Marzougui, A.; Kostick, S.; Si, Y.; Quirós Vargas, J.J.; Evans, K. High-throughput phenotyping of fire blight disease symptoms using sensing techniques in apple. *Front. Plant Sci.* **2019**, *10*, 576. [[CrossRef](#)] [[PubMed](#)]
104. Qiu, T.; Underhill, A.; Sapkota, S.; Cadle-Davidson, L.; Jiang, Y. High throughput saliency-based quantification of grape powdery mildew at the microscopic level for disease resistance breeding. *Hortic. Res.* **2022**, *9*, uhac187. [[CrossRef](#)] [[PubMed](#)]
105. Sultan Mahmud, M.; Zaman, Q.U.; Esau, T.J.; Price, G.W.; Prithiviraj, B. Development of an artificial cloud lighting condition system using machine vision for strawberry powdery mildew disease detection. *Comput. Electron. Agric.* **2019**, *158*, 219–225. [[CrossRef](#)]
106. Tapia, R.; Abd-Elrahman, A.; Osorio, L.; Lee, S.; Whitaker, V.M. Combining canopy reflectance spectrometry and genome-wide prediction to increase response to selection for powdery mildew resistance in cultivated strawberry. *J. Exp. Bot.* **2022**, *73*, 5322–5335. [[CrossRef](#)] [[PubMed](#)]
107. Elliott, K.; Berry, J.C.; Kim, H.; Bart, R.S. A comparison of ImageJ and machine learning based image analysis methods to measure cassava bacterial blight disease severity. *Plant Methods* **2022**, *18*, 86. [[CrossRef](#)]
108. Kim, J.H.; Bhandari, S.R.; Chae, S.Y.; Cho, M.C.; Lee, J.G. Application of maximum quantum yield, a parameter of chlorophyll fluorescence, for early determination of bacterial wilt in tomato seedlings. *Hortic. Environ. Biotechnol.* **2019**, *60*, 821–829. [[CrossRef](#)]
109. Kundu, R.; Dutta, D.; MK, N.; Chakrabarty, A. Near Real Time Monitoring of Potato Late Blight Disease Severity using Field Based Hyperspectral Observation. *Smart Agric. Technol.* **2021**, *1*, 100019. [[CrossRef](#)]
110. Hou, C.; Zhuang, J.; Tang, Y.; He, Y.; Miao, A.; Huang, H.; Luo, S. Recognition of early blight and late blight diseases on potato leaves based on graph cut segmentation. *J. Agric. Food Res.* **2021**, *5*, 100154. [[CrossRef](#)]
111. Franceschini, M.H.D.; Bartholomeus, H.; van Apeldoorn, D.F.; Suomalainen, J.; Kooistra, L. Feasibility of unmanned aerial vehicle optical imagery for early detection and severity assessment of late blight in Potato. *Remote Sens.* **2019**, *11*, 224. [[CrossRef](#)]
112. Virlet, N.; Costes, E.; Martinez, S.; Kelner, J.J.; Regnard, J.L. Multispectral airborne imagery in the field reveals genetic determinisms of morphological and transpiration traits of an apple tree hybrid population in response to water deficit. *J. Exp. Bot.* **2015**, *66*, 5453–5465. [[CrossRef](#)]
113. Briglia, N.; Montanaro, G.; Petrozza, A.; Summerer, S.; Cellini, F.; Nuzzo, V. Drought phenotyping in *Vitis vinifera* using RGB and NIR imaging. *Sci. Hortic.* **2019**, *256*, 108555. [[CrossRef](#)]
114. Chen, S.; Guo, Y.; Sirault, X.; Stefanova, K.; Saradadevi, R.; Turner, N.C.; Nelson, M.N.; Furbank, R.T.; Siddique, K.H.M.; Cowling, W.A. Nondestructive phenomic tools for the prediction of heat and drought tolerance at anthesis in Brassica species. *Plant Phenom.* **2019**, *2019*, 3264872. [[CrossRef](#)] [[PubMed](#)]
115. Faqeerzada, M.A.; Park, E.; Kim, T.; Kim, M.S.; Baek, I.; Joshi, R.; Kim, J.; Cho, B.K. Fluorescence Hyperspectral Imaging for Early Diagnosis of Heat-Stressed Ginseng Plants. *Appl Sci.* **2023**, *13*, 31.
116. Zea, M.; Souza, A.; Yang, Y.; Lee, L.; Nemali, K.; Hoagland, L. Leveraging high-throughput hyperspectral imaging technology to detect cadmium stress in two leafy green crops and accelerate soil remediation efforts. *Environ. Pollut.* **2022**, *292*, 118405. [[CrossRef](#)] [[PubMed](#)]
117. Ropelewska, E.; Rutkowski, K.P. Cultivar discrimination of stored apple seeds based on geometric features determined using image analysis. *J. Stored Prod. Res.* **2021**, *92*, 101804. [[CrossRef](#)]
118. Wu, J.; Yang, G.; Yang, H.; Zhu, Y.; Li, Z.; Lei, L.; Zhao, C. Extracting apple tree crown information from remote imagery using deep learning. *Comput. Electron. Agric.* **2020**, *174*, 105504. [[CrossRef](#)]
119. Sun, X.; Fang, W.; Gao, C.; Fu, L.; Majeed, Y.; Liu, X.; Gao, F.; Yang, R.; Li, R. Remote estimation of grafted apple tree trunk diameter in modern orchard with RGB and point cloud based on SOLOv. *Comput. Electron. Agric.* **2022**, *199*, 107209. [[CrossRef](#)]
120. Fu, L.; Majeed, Y.; Zhang, X.; Karkee, M.; Zhang, Q. Faster R-CNN-based apple detection in dense-foilage fruiting-wall trees using RGB and depth features for robotic harvesting. *Biosyst. Eng.* **2020**, *197*, 245–256. [[CrossRef](#)]
121. Chen, W.; Zhang, J.; Guo, B.; Wei, Q.; Zhu, Z. An Apple Detection Method Based on Des-YOLO v4 Algorithm for Harvesting Robots in Complex Environment. *Math. Probl. Eng.* **2021**, *2021*, 7351470. [[CrossRef](#)]
122. Ge, L.; Zou, K.; Zhou, H.; Yu, X.; Tan, Y.; Zhang, C.; Li, W. Three dimensional apple tree organs classification and yield estimation algorithm based on multi-features fusion and support vector machine. *Inf. Process. Agric.* **2022**, *9*, 431–442. [[CrossRef](#)]
123. Sabzi, S.; Abbaspour-Gilandeh, Y.; García-Mateos, G.; Ruiz-Canales, A.; Molina-Martínez, J.M.; Arribas, J.I. An automatic non-destructive method for the classification of the ripeness stage of red delicious apples in orchards using aerial video. *Agronomy* **2019**, *9*, 84. [[CrossRef](#)]
124. Shurygin, B.; Konyukhov, I.; Khrushev, S.; Solovchenko, A. Non-Invasive Probing of Winter Dormancy via Time-Frequency Analysis of Induced Chlorophyll Fluorescence in Deciduous Plants as Exemplified by Apple (*Malus × domestica* Borkh.). *Plants* **2022**, *11*, 2811. [[CrossRef](#)] [[PubMed](#)]
125. Schlie, T.P.; Dierend, W.; Köpcke, D.; Rath, T. Detecting low-oxygen stress of stored apples using chlorophyll fluorescence imaging and histogram division. *Postharvest. Biol. Technol.* **2022**, *189*, 111901. [[CrossRef](#)]
126. Miao, Y.; Wang, L.; Peng, C.; Li, H.; Li, X.; Zhang, M. Banana plant counting and morphological parameters measurement based on terrestrial laser scanning. *Plant Methods* **2022**, *18*, 66. [[CrossRef](#)]

127. Huang, K.Y.; Cheng, J.F. A novel auto-sorting system for Chinese cabbage seeds. *Sensors* **2017**, *17*, 886. [[CrossRef](#)]
128. Turner, S.D.; Ellison, S.L.; Senalik, D.A.; Simon, P.W.; Spalding, E.P.; Miller, N.D. An automated image analysis pipeline enables genetic studies of shoot and root morphology in carrot (*Daucus carota* L.). *Front. Plant Sci.* **2018**, *871*, 1703. [[CrossRef](#)]
129. Brainard, S.H.; Ellison, S.L.; Simon, P.W.; Dawson, J.C.; Goldman, I.L. Genetic characterization of carrot root shape and size using genome-wide association analysis and genomic-estimated breeding values. *Theor. Appl. Genet.* **2022**, *135*, 605–622. [[CrossRef](#)]
130. Delgado, A.; Hays, D.B.; Bruton, R.K.; Ceballos, H.; Novo, A.; Boi, E.; Selvaraj, M.G. Ground penetrating radar: A case study for estimating root bulking rate in cassava (*Manihot esculenta* Crantz). *Plant Methods* **2017**, *13*, 65. [[CrossRef](#)]
131. Yonis, B.O.; Pino del Carpio, D.; Wolfe, M.; Jannink, J.L.; Kulakow, P.; Rabbi, I. Improving root characterisation for genomic prediction in cassava. *Sci. Rep.* **2020**, *10*, 8003. [[CrossRef](#)]
132. Atanbori, J.; Montoya, P.M.E.; Selvaraj, M.G.; French, A.P.; Pridmore, T.P. Convolutional Neural Net-Based Cassava Storage Root Counting Using Real and Synthetic Images. *Front. Plant Sci.* **2019**, *10*, 1516. [[CrossRef](#)]
133. Agbona, A.; Teare, B.; Ruiz-Guzman, H.; Dobрева, I.D.; Everett, M.E.; Adams, T.; Montesinos-Lopez, O.A.; Kulakow, P.A.; Hays, D.B. Prediction of root biomass in cassava based on ground penetrating radar phenomics. *Remote Sens.* **2021**, *13*, 4908. [[CrossRef](#)]
134. Nkouaya Mbanjo, E.G.; Hershberger, J.; Peteti, P.; Agbona, A.; Ikpan, A.; Ogunpaimo, K.; Kayondo, S.I.; Abioye, R.S.; Nafiu, K.; Alamu, E.O.; et al. Predicting starch content in cassava fresh roots using near-infrared spectroscopy. *Front. Plant Sci.* **2022**, *13*, 990250. [[CrossRef](#)] [[PubMed](#)]
135. Selvaraj, M.G.; Valderrama, M.; Guzman, D.; Valencia, M.; Ruiz, H.; Acharjee, A. Machine learning for high-throughput field phenotyping and image processing provides insight into the association of above and below-ground traits in cassava (*Manihot esculenta* Crantz). *Plant Methods* **2020**, *16*, 87. [[CrossRef](#)] [[PubMed](#)]
136. Csillik, O.; Cherbini, J.; Johnson, R.; Lyons, A.; Kelly, M. Identification of citrus trees from unmanned aerial vehicle imagery using convolutional neural networks. *Drones* **2018**, *2*, 39. [[CrossRef](#)]
137. Osco, L.P.; de Arruda, M.D.S.; Marcato Junior, J.; da Silva, N.B.; Ramos, A.P.M.; Moryia, É.A.S.; Imai, N.N.; Pereira, D.R.; Creste, J.E.; Matsubara, E.T.; et al. A convolutional neural network approach for counting and geolocating citrus-trees in UAV multispectral imagery. *ISPRS J. Photogramm. Remote Sens.* **2020**, *160*, 97–106. [[CrossRef](#)]
138. Zhang, X.; Derival, M.; Albrecht, U.; Ampatzidis, Y. Evaluation of a ground penetrating radar to map the root architecture of HLB-infected citrus trees. *Agronomy* **2019**, *9*, 354. [[CrossRef](#)]
139. Chang, A.; Yeom, J.; Jung, J.; Landivar, J. Comparison of canopy shape and vegetation indices of citrus trees derived from UAV multispectral images for characterization of citrus greening disease. *Remote Sens.* **2020**, *12*, 4122. [[CrossRef](#)]
140. Rist, F.; Herzog, K.; Mack, J.; Richter, R.; Steinhage, V.; Töpfer, R. High-precision phenotyping of grape bunch architecture using fast 3d sensor and automation. *Sensors* **2018**, *18*, 763. [[CrossRef](#)] [[PubMed](#)]
141. Rist, F.; Gabriel, D.; Mack, J.; Steinhage, V.; Töpfer, R.; Herzog, K. Combination of an automated 3D field phenotyping workflow and predictive modelling for high-throughput and non-invasive phenotyping of grape bunches. *Remote Sens.* **2019**, *11*, 2953. [[CrossRef](#)]
142. Luo, L.; Liu, W.; Lu, Q.; Wang, J.; Wen, W.; Yan, D.; Tang, Y. Grape berry detection and size measurement based on edge image processing and geometric morphology. *Machines* **2021**, *9*, 233. [[CrossRef](#)]
143. Liu, S.; Zeng, X.; Whitty, M. A vision-based robust grape berry counting algorithm for fast calibration-free bunch weight estimation in the field. *Comput. Electron. Agric.* **2020**, *173*, 105360. [[CrossRef](#)]
144. Buayai, P.; Saikaew, K.R.; Mao, X. End-to-End Automatic Berry Counting for Table Grape Thinning. *IEEE Access* **2021**, *9*, 4829–4842. [[CrossRef](#)]
145. Ramos, R.P.; Gomes, J.S.; Prates, R.M.; Simas Filho, E.F.; Teruel, B.J.; dos Santos Costa, D. Non-invasive setup for grape maturation classification using deep learning. *J. Sci. Food Agric.* **2021**, *101*, 2042–2051. [[CrossRef](#)] [[PubMed](#)]
146. Anastasiou, E.; Balafoutis, A.; Darra, N.; Psiroukis, V.; Biniari, A.; Xanthopoulos, G.; Fountas, S. Satellite and proximal sensing to estimate the yield and quality of table grapes. *Agriculture* **2018**, *8*, 94. [[CrossRef](#)]
147. Torres-Sánchez, J.; Mesas-Carrascosa, F.J.; Santesteban, L.G.; Jiménez-Brenes, F.M.; Oñeka, O.; Villa-Llop, A.; Loidi, M.; López-Granados, F. Grape cluster detection using UAV photogrammetric point clouds as a low-cost tool for yield forecasting in vineyards. *Sensors* **2021**, *21*, 3083. [[CrossRef](#)]
148. Olenskyj, A.G.; Sams, B.S.; Fei, Z.; Singh, V.; Raja, P.V.; Bornhorst, G.M.; Earles, J.M. End-to-end deep learning for directly estimating grape yield from ground-based imagery. *Comput. Electron. Agric.* **2022**, *198*, 107081. [[CrossRef](#)]
149. Gao, Z.; Khot, L.R.; Naidu, R.A.; Zhang, Q. Early detection of grapevine leafroll disease in a red-berried wine grape cultivar using hyperspectral imaging. *Comput. Electron. Agric.* **2020**, *179*, 105807. [[CrossRef](#)]
150. Seki, K.; Toda, Y. QTL mapping for seed morphology using the instance segmentation neural network in *Lactuca* spp. *Front. Plant Sci.* **2022**, *13*, 949470. [[CrossRef](#)]
151. Du, J.; Li, B.; Lu, X.; Yang, X.; Guo, X.; Zhao, C. Quantitative phenotyping and evaluation for lettuce leaves of multiple semantic components. *Plant Methods* **2022**, *18*, 54. [[CrossRef](#)]
152. Du, J.; Lu, X.; Fan, J.; Qin, Y.; Yang, X.; Guo, X. Image-Based High-Throughput Detection and Phenotype Evaluation Method for Multiple Lettuce Varieties. *Front. Plant Sci.* **2020**, *11*, 563386. [[CrossRef](#)]
153. Zhang, L.; Xu, Z.; Xu, D.; Ma, J.; Chen, Y.; Fu, Z. Growth monitoring of greenhouse lettuce based on a convolutional neural network. *Hortic. Res.* **2020**, *7*, 124.

154. Kim, C.; van Iersel, M.W. Morphological and Physiological Screening to Predict Lettuce Biomass Production in Controlled Environment Agriculture. *Remote Sens.* **2022**, *14*, 316. [[CrossRef](#)]
155. Zhang, Y.; Li, M.; Li, G.; Li, J.; Zheng, L.; Zhang, M.; Wang, M. Multi-phenotypic parameters extraction and biomass estimation for lettuce based on point clouds. *Measurement* **2022**, *204*, 112094. [[CrossRef](#)]
156. Maciel, G.M.; Gallis, R.B.A.; Barbosa, R.L.; Pereira, L.M.; Siquieroli, A.C.S.; Peixoto, J.V.M. Image phenotyping of lettuce germplasm with genetically diverse carotenoid levels. *Bragantia* **2020**, *79*, 224–235. [[CrossRef](#)]
157. Osco, L.P.; Ramos, A.P.M.; Moriya, É.A.S.; Bavaresco, L.G.; de Lima, B.C.; Estrabis, N.; Pereira, D.R.; Creste, J.E.; Júnior, J.M.; Gonçalves, W.N.; et al. Modeling hyperspectral response of water-stress induced lettuce plants using artificial neural networks. *Remote Sens.* **2019**, *11*, 2797. [[CrossRef](#)]
158. Sorrentino, M.; Colla, G.; Roupheal, Y.; Panzarová, K.; Trtílek, M. Lettuce reaction to drought stress: Automated high-throughput phenotyping of plant growth and photosynthetic performance. *Acta Hort.* **2020**, *1268*, 133–141. [[CrossRef](#)]
159. Wendel, A.; Underwood, J.; Walsh, K. Maturity estimation of mangoes using hyperspectral imaging from a ground based mobile platform. *Comput. Electron. Agric.* **2018**, *155*, 298–313. [[CrossRef](#)]
160. Guo, Y.; Chen, S.; Wu, Z.; Wang, S.; Bryant, C.R.; Senthilnath, J.; Cunha, M.; Fu, Y.H. Integrating spectral and textural information for monitoring the growth of pear trees using optical images from the UAV platform. *Remote Sens.* **2021**, *13*, 1795. [[CrossRef](#)]
161. Raju Ahmed, M.; Yasmin, J.; Wakholi, C.; Mukasa, P.; Cho, B.K. Classification of pepper seed quality based on internal structure using X-ray CT imaging. *Comput. Electron. Agric.* **2020**, *179*, 105839. [[CrossRef](#)]
162. Horgan, G.W.; Song, Y.; Glasbey, C.A.; Van Der Heijden, G.W.A.M.; Polder, G.; Dieleman, J.A.; Bink, M.C.A.M.; Van Eeuwijk, F.A. Automated estimation of leaf area development in sweet pepper plants from image analysis. *Funct. Plant Biol.* **2015**, *42*, 486–492. [[CrossRef](#)]
163. Musse, M.; Hajjar, G.; Ali, N.; Billiot, B.; Joly, G.; Pépin, J.; Quéllec, S.; Challos, S.; Mariette, F.; Cambert, M.; et al. A global non-invasive methodology for the phenotyping of potato under water deficit conditions using imaging, physiological and molecular tools. *Plant Methods* **2021**, *17*, 81. [[CrossRef](#)] [[PubMed](#)]
164. Van Harselaar, J.K.; Claußen, J.; Lübeck, J.; Wörlein, N.; Uhlmann, N.; Sonnewald, U.; Gerth, S. X-ray CT Phenotyping Reveals Bi-Phasic Growth Phases of Potato Tubers Exposed to Combined Abiotic Stress. *Front. Plant Sci.* **2021**, *12*, 613108. [[CrossRef](#)] [[PubMed](#)]
165. Caraza-Harter, M.V.; Endelman, J.B. Image-based phenotyping and genetic analysis of potato skin set and color. *Crop Sci.* **2020**, *60*, 202–210. [[CrossRef](#)]
166. Si, Y.; Sankaran, S.; Knowles, N.R.; Pavek, M.J. Potato Tuber Length-Width Ratio Assessment Using Image Analysis. *Am. J. Potato Res.* **2017**, *94*, 88–93. [[CrossRef](#)]
167. Yang, H.; Li, F.; Wang, W.; Yu, K. Estimating above-ground biomass of potato using random forest and optimized hyperspectral indices. *Remote Sens.* **2021**, *13*, 2339. [[CrossRef](#)]
168. Liu, Y.; Feng, H.; Yue, J.; Fan, Y.; Jin, X.; Song, X.; Yang, H.; Yang, G. Estimation of Potato Above-Ground Biomass Based on Vegetation Indices and Green-Edge Parameters Obtained from UAVs. *Remote Sens.* **2022**, *14*, 5323. [[CrossRef](#)]
169. Fan, Y.; Feng, H.; Jin, X.; Yue, J.; Liu, Y.; Li, Z.; Feng, Z.; Song, X.; Yang, G. Estimation of the nitrogen content of potato plants based on morphological parameters and visible light vegetation indices. *Front. Plant Sci.* **2022**, *13*, 1012070. [[CrossRef](#)]
170. Muruganatham, P.; Samrat, N.H.; Islam, N.; Johnson, J.; Wibowo, S.; Grandhi, S. Rapid Estimation of Moisture Content in Unpeeled Potato Tubers Using Hyperspectral Imaging. *Appl. Sci.* **2023**, *13*, 53. [[CrossRef](#)]
171. Sun, C.; Feng, L.; Zhang, Z.; Ma, Y.; Crosby, T.; Naber, M.; Wang, Y. Prediction of end-of-season tuber yield and tuber set in potatoes using in-season UAV-based hyperspectral imagery and machine learning. *Sensors* **2020**, *20*, 5293. [[CrossRef](#)]
172. Van De Vijver, R.; Mertens, K.; Heungens, K.; Somers, B.; Nuyttens, D.; Borra-Serrano, I.; Lootens, P.; Roldán-Ruiz, I.; Vangeyte, J.; Saeys, W. In-field detection of *Alternaria solani* in potato crops using hyperspectral imaging. *Comput. Electron. Agric.* **2020**, *168*, 105106. [[CrossRef](#)]
173. Duarte-Carvajalino, J.M.; Alzate, D.F.; Ramirez, A.A.; Santa-Sepulveda, J.D.; Fajardo-Rojas, A.E.; Soto-Suárez, M. Evaluating late blight severity in potato crops using unmanned aerial vehicles and machine learning algorithms. *Remote Sens.* **2018**, *10*, 1513. [[CrossRef](#)]
174. Qi, C.; Sandroni, M.; Cairo Westergaard, J.; Høegh Riis Sundmark, E.; Bagge, M.; Alexandersson, E.; Gao, J. In-field classification of the asymptomatic biotrophic phase of potato late blight based on deep learning and proximal hyperspectral imaging. *Comput. Electron. Agric.* **2023**, *205*, 107585. [[CrossRef](#)]
175. Saha, K.K.; Tsoulias, N.; Weltzien, C.; Zude-Sasse, M. Estimation of Vegetative Growth in Strawberry Plants Using Mobile LiDAR Laser Scanner. *Horticulturae* **2022**, *8*, 90. [[CrossRef](#)]
176. Feldmann, M.J.; Hardigan, M.A.; Famula, R.A.; López, C.M.; Tabb, A.; Cole, G.S.; Knapp, S.J. Multi-dimensional machine learning approaches for fruit shape phenotyping in strawberry. *GigaScience* **2020**, *9*, g1aa030. [[CrossRef](#)] [[PubMed](#)]
177. Zingaretti, L.M.; Monfort, A.; Pérez-Enciso, M. Automatic fruit morphology phenome and genetic analysis: An application in the octoploid strawberry. *Plant Phenom.* **2021**, *2021*, 981291. [[CrossRef](#)]
178. Li, B.; Cockerton, H.M.; Johnson, A.W.; Karlström, A.; Stavridou, E.; Deakin, G.; Harrison, R.J. Defining strawberry shape uniformity using 3D imaging and genetic mapping. *Hortic. Res.* **2020**, *7*, 115. [[CrossRef](#)]
179. Zheng, C.; Abd-Elrahman, A.; Whitaker, V.M.; Dalid, C. Deep Learning for Strawberry Canopy Delineation and Biomass Prediction from High-Resolution Images. *Plant Phenom.* **2022**, *2022*, 9850486. [[CrossRef](#)]

180. Guan, Z.; Abd-Elrahman, A.; Fan, Z.; Whitaker, V.M.; Wilkinson, B. Modeling strawberry biomass and leaf area using object-based analysis of high-resolution images. *ISPRS J. Photogramm. Remote Sens.* **2020**, *163*, 171–186. [[CrossRef](#)]
181. Cockerton, H.M.; Li, B.; Vickerstaff, R.J.; Eyre, C.A.; Sargent, D.J.; Armitage, A.D.; Marina-Montes, C.; Garcia-Cruz, A.; Passey, A.J.; Simpson, D.W.; et al. Identifying *Verticillium dahliae* Resistance in Strawberry Through Disease Screening of Multiple Populations and Image Based Phenotyping. *Front. Plant Sci.* **2019**, *10*, 924. [[CrossRef](#)]
182. Poobalalabramanian, M.; Park, E.S.; Faqeerzada, M.A.; Kim, T.; Kim, M.S.; Baek, I.; Cho, B.K. Identification of Early Heat and Water Stress in Strawberry Plants Using Chlorophyll-Fluorescence Indices Extracted via Hyperspectral Images. *Sensors* **2022**, *22*, 8706. [[CrossRef](#)]
183. Zhu, Y.; Gu, Q.; Zhao, Y.; Wan, H.; Wang, R.; Zhang, X.; Cheng, Y. Quantitative Extraction and Evaluation of Tomato Fruit Phenotypes Based on Image Recognition. *Front. Plant Sci.* **2022**, *13*, 859290. [[CrossRef](#)] [[PubMed](#)]
184. Sun, G.; Wang, X.; Sun, Y.; Ding, Y.; Lu, W. Measurement method based on multispectral three-dimensional imaging for the chlorophyll contents of greenhouse tomato plants. *Sensors* **2019**, *19*, 3345. [[CrossRef](#)] [[PubMed](#)]
185. Chang, A.; Jung, J.; Yeom, J.; Maeda, M.M.; Landivar, J.A.; Enciso, J.M.; Avila, C.A.; Anciso, J.R. Unmanned Aircraft System-(UAS-) Based High-Throughput Phenotyping (HTP) for Tomato Yield Estimation. *J. Sens.* **2021**, *2021*, 8875606. [[CrossRef](#)]
186. Tatsumi, K.; Igarashi, N.; Mengxue, X. Prediction of plant-level tomato biomass and yield using machine learning with unmanned aerial vehicle imagery. *Plant Methods* **2021**, *17*, 77. [[CrossRef](#)]
187. Méline, V.; Caldwell, D.L.; Kim, B.S.; Khangura, R.S.; Baireddy, S.; Yang, C.; Sparks, E.E.; Dilkes, B.; Delp, E.J.; Iyer-Pascuzzi, A.S. Image-based assessment of plant disease progression identifies new genetic loci for resistance to *Ralstonia solanacearum* in tomato. *Plant J.* **2023**, *113*, 887–903. [[CrossRef](#)] [[PubMed](#)]
188. Žibrat, U.; Susič, N.; Knapič, M.; Širc, S.; Strajnar, P.; Razinger, J.; Vončina, A.; Urek, G.; Gerič Stare, B. Pipeline for imaging, extraction, pre-processing, and processing of time-series hyperspectral data for discriminating drought stress origin in tomatoes. *MethodsX* **2019**, *6*, 399–408. [[CrossRef](#)] [[PubMed](#)]
189. Fullana-Pericàs, M.; Conesa, M.À.; Gago, J.; Ribas-Carbó, M.; Galmés, J. High-throughput phenotyping of a large tomato collection under water deficit: Combining UAVs' remote sensing with conventional leaf-level physiologic and agronomic measurements. *Agric. Water Manag.* **2022**, *260*, 107283. [[CrossRef](#)]
190. Tsaftaris, S.A.; Minervini, M.; Schar, H. Machine Learning for Plant Phenotyping Needs Image Processing. *Trends Plant Sci.* **2016**, *21*, 989–991. [[CrossRef](#)]
191. Mochida, K.; Koda, S.; Inoue, K.; Hirayama, T.; Tanaka, S.; Nishii, R.; Melgani, F. Computer vision-based phenotyping for improvement of plant productivity: A machine learning perspective. *GigaScience* **2019**, *8*, giy153. [[CrossRef](#)]
192. Yoosefzadeh-Najafabadi, M.; Earl, H.J.; Tulpan, D.; Sulik, J.; Eskandari, M. Application of Machine Learning Algorithms in Plant Breeding: Predicting Yield from Hyperspectral Reflectance in Soybean. *Front. Plant Sci.* **2021**, *11*, 624273. [[CrossRef](#)]
193. Khan, M.; Jan, B.; Farman, H. *Deep Learning: Convergence to Big Data Analytics*, 1st ed.; SpringerBriefs in Computer Science; Springer: Singapore, 2019.
194. LeCun, Y.; Bengio, Y.; Hinton, G. Deep learning. *Nature* **2015**, *521*, 436–444. [[CrossRef](#)] [[PubMed](#)]
195. Kim, Y.; Kwak, G.-H.; Lee, K.-D.; Na, S.-I.; Park, C.-W.; Park, N.-W. Performance Evaluation of Machine Learning and Deep Learning Algorithms in Crop Classification: Impact of Hyper-parameters and Training Sample Size. *Korean J. Remote Sens.* **2018**, *34*, 811–827.
196. Toda, Y.; Okura, F.; Ito, J.; Okada, S.; Kinoshita, T.; Tsuji, H.; Saisho, D. Training instance segmentation neural network with synthetic datasets for crop seed phenotyping. *Commun. Biol.* **2020**, *3*, 173. [[CrossRef](#)] [[PubMed](#)]
197. Singh, A.K.; Ganapathysubramanian, B.; Sarkar, S.; Singh, A. Deep Learning for Plant Stress Phenotyping: Trends and Future Perspectives. *Trends Plant Sci.* **2018**, *23*, 883–898. [[CrossRef](#)] [[PubMed](#)]
198. Ubbens, J.R.; Stavness, I. Deep Plant Phenomics: A Deep Learning Platform for Complex Plant Phenotyping Tasks. *Front. Plant Sci.* **2017**, *8*, 1190. [[CrossRef](#)]

Disclaimer/Publisher's Note: The statements, opinions and data contained in all publications are solely those of the individual author(s) and contributor(s) and not of MDPI and/or the editor(s). MDPI and/or the editor(s) disclaim responsibility for any injury to people or property resulting from any ideas, methods, instructions or products referred to in the content.